

**PAC29 Proposal for the Extension of the g7
Experiment (g7b)**

**“Search for Modification of Vector Meson
Properties in Nuclei”**

D. P. Weygand (spokesperson - contact person¹), L. Guo
Jefferson Laboratory, Newport News, VA 23606

C. Djalali (spokesperson), R. Nasseripour (spokesperson),
R. Gothe, D. Tedeschi, S. Strauch
University of South Carolina, Columbia, SC 29208

M. H. Wood (spokesperson), R. Miskimen
University of Massachusetts, Amherst

and the CLAS Collaboration

December 5, 2005

¹Email: weygand@jlab.org, Ph: (757)269-5926, Fax: (757)269-5800

Contents

1	Physics Motivations	2
1.1	In-Medium Hadron Modifications	2
1.2	Prediction of Theoretical Models	3
1.3	Existing Data	5
1.4	Advantages of g7 Experiment	12
2	Manpower	16
3	Feasibility– Analysis of g7(a) data	18
3.1	Lepton Pair Identification	18
3.2	Momentum and Target Energy Loss Corrections	21
3.3	Simulations and Detector Acceptance	22
3.4	g7a results	29
4	g7b Running Conditions	33
4.1	Data Rate	33
4.2	Trigger	35
4.3	g7b Simulations	35
4.4	Background Rates	40
4.5	g7b Target Geometry	42
4.6	Photon Beam Energy	42
4.7	Magnetic field settings to optimize the ϕ meson study	44
5	Summary	48
6	Acknowledgment	49

List of Figures

1	CERES result.	4
2	Prediction of models.	5
3	TAGX result.	6
4	KEK result.	7
5	KEK result.	8
6	TAPS result.	9
7	PHENIX result.	9
8	CERN SPS result.	10
9	z-component of vertex position	13
10	EC cuts for electrons.	19
11	EC cuts for positrons.	20
12	Number of photoelectrons in the CC.	21
13	Electron SC time versus positron SC time.	22
14	Vertex timing cut for e^- and e^+	23
15	Comparison of vertex timing for e^- and π^-	25
16	Mixed Background.	26
17	Detector Acceptance.	27
18	Compton and pair production simulations.	28
19	g7a result, D2 target.	30
20	g7a result, C target.	30
21	g7a result, Fe-Ti target.	31
22	g7a result, Pb target.	31
23	Significant of the fits.	32
24	DVCS solenoid simulation geometry.	37
25	g7b Simulation with no DVCS solenoid magnet.	38
26	g7b Simulation with DVCS solenoid magnet.	39
27	Single lepton trigger rate for g7a data.	40
28	Two lepton trigger rate for g7a data.	41

29	Beam energy for ϕ production.	43
30	Lepton momentum versus polar angle.	45
31	e^+e^- pair momentum versus invariant mass.	46
32	Simulation with various torus settings and target positions.	47

Abstract

We propose an extension to the g7a experiment (g7b) with a photon beam up to 3 GeV on a set of nuclear targets (D₂, C, Fe, Nb) using CLAS detector. The goal of the g7a/b experiment is to study the in-medium modifications in the mass and/or width of the light vector mesons, ρ , ω , and ϕ via their rare leptonic decay. This decay channel is preferred over the hadronic modes in order to eliminate the final state interaction in the nuclear matter. The in-medium modifications can be related to more fundamental physics such as partial restoration of chiral symmetry at high density.

The result of g7a experiment has demonstrated the ability of CLAS detector to detect the e^+e^- decay of all the three vector mesons. The result of the fits (with and without medium modification) to the g7a data favor a downward shift in the mass of the ρ meson. However, it is not possible to draw any statistically significant conclusion. The extension of the g7a experiment (g7b) is proposed to increase the statistics. The primary goal of the g7a/b experiment is to study the ρ meson. The main strength is the ρ which is clearly seen in all the targets. Increasing amount of data by a factor of 4 to 5 will allow at the 99% confidence level an observation of the mass shift greater than 20 MeV. A secondary goal is to study of the ϕ meson which would require 10 times the statistics to be sensitive to the ϕ meson decaying inside the nucleus. The increase in statistics needed for the study of the ρ meson can be done safely by increasing the instantaneous luminosity over g7a ($\times 2-2.5$) and running time to 36 days.

In order to reduce the amount of the background we plan to replace the Pb with Nb target and study the possibility of using the DVCS solenoid instead of the mini-torus. The unique characteristics of g7a/b experiment: an electromagnetic probe and a final state unhindered by strong interactions provides a direct measurement of the vector meson properties in the medium.

1 Physics Motivations

1.1 In-Medium Hadron Modifications

Quantum Chromodynamics (QCD), the theory of the strong interaction, has been remarkably successful in describing high-energy and short-distance-scale experiments involving quarks and gluons. However, applying QCD to low energy and large-distance-scale experiments has been a major challenge. Although the rapidly increasing strength of the interaction in this latter case makes it impossible to apply perturbative techniques, the symmetries of QCD (such as chiral symmetry) provide guiding principles to deal with strong interaction phenomena. Various QCD-inspired predictions are now available in the non-perturbative domain, which can be tested experimentally at current hadron and electromagnetic facilities.

One of these QCD “inspired” predictions is that in hot (finite temperature) and/or dense (finite density) matter, a chiral phase transition takes place and the broken chiral symmetry is restored resulting in a modification of the properties of hadrons (vector mesons in particular) in nuclear matter from their free-space values. This prediction has generated much interest, and there is an urgent need for experimental data to confirm or refute these predictions in this as yet largely unexplored domain. The first evidence as to the possibility of a medium-lowered ρ meson mass came from the CERES and HELIOS/3 collaborations of CERN in 1995 [1, 2]. The CERES collaboration reported on measurements of low-mass e^+e^- pairs from p-Au and Pb-Au collisions (Fig. 1). Di-lepton spectroscopy allows measurement of the in-medium properties without distortion due to final state interactions (FSI). While their proton-induced data could satisfactorily be accounted for by summing various hadron decay contributions, an enhancement over the hadronic contributions was observed for the Pb-Au data in the mass range between 300 and 700 (MeV/ c^2). The same year, theorists were able to account for this excess by using a relativistic transport model assuming a drop in the mass of the ρ meson [3]. It has been suggested that traditional effects, such as an in-medium modified pion dispersion relation may be able to provide enough enhancement [4, 5]. A better understanding

of hadron properties in a hot and/or dense environment is therefore one of the most important endeavors of hadronic physics today. The change of properties of the vector mesons in the medium is a hot topic that is currently being studied at RHIC (BNL) and HADES (GSI) and will be studied at ALICE (CERN) by measuring low mass di-lepton production. Although vector mesons preferentially decay into pions, the large final state interactions of the pions with the nuclear medium makes it almost impossible to derive any direct information about the meson properties in the medium. In a heavy-ion collision the final di-lepton yield is obtained by an integration over different densities and temperatures, and a discrimination between different scenarios of the in-medium modifications for the vector mesons is difficult. In their initial stages, relativistic heavy-ion reactions originate far from equilibrium and the temperature and density evolve over time. However, all theoretical predictions of in-medium properties of vector mesons in photon or pion induced reactions allow one to study the hadron properties in an environment that is much closer to equilibrium (normal nuclear density and zero temperature). The predicted in-medium effects for the vector mesons by the different models are so large that they should have observable consequences already at normal nuclear density.

An experiment like g7 at Jlab is ideal to measure the photoproduction of vector mesons off nuclei and will give complementary information about the in-medium properties of mesons.

1.2 Prediction of Theoretical Models

Due to chiral symmetry restoration, the mass and width of vector mesons, ω , ρ , and ϕ , are predicted to change with increasing density. Brown and Rho [6], starting from an effective Lagrangian approach at low energy and zero density, suggest the same Lagrangian at high density, but with the masses and coupling constants that are modified according to the symmetry constraints of QCD. They proposed an in-medium scaling law that predicts a decrease in the mass of the vector meson by

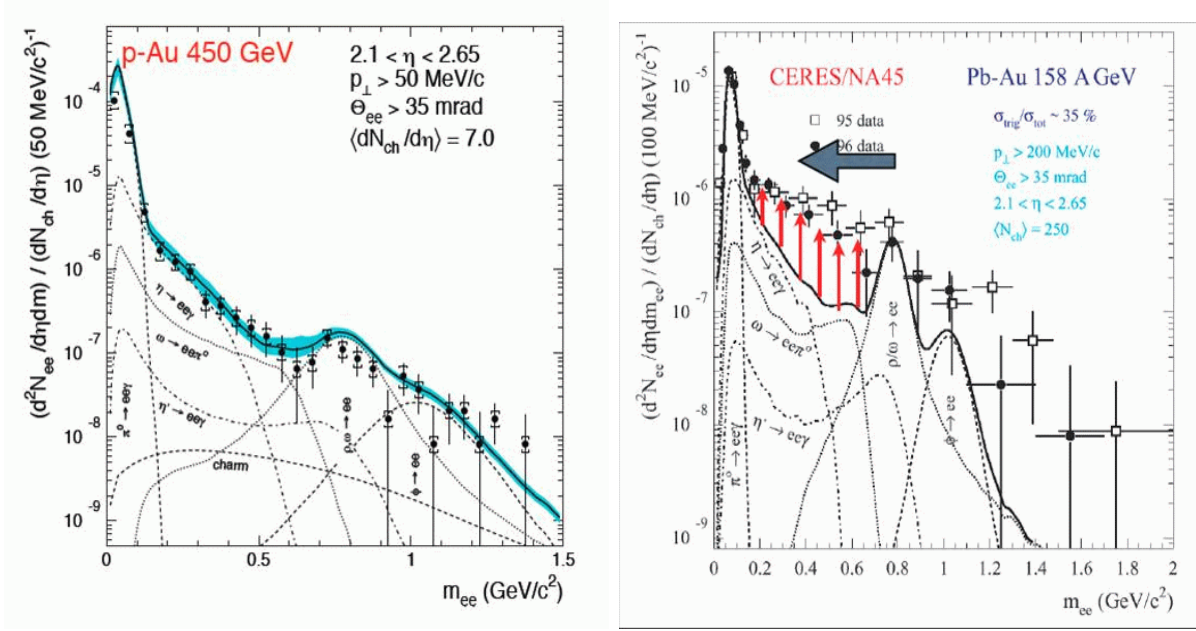


Figure 1: CERES result. Inclusive e^+e^- mass spectra in 450 GeV p-Au (left) and 200 GeV Pb-Au (right) collisions showing the data (full circles) and the various contributions from hadronic decays. The shaded regions indicate the systematic error on the summed contributions.

about 20%:

$$\frac{m_{VM}(\rho_0)}{m_{VM}(\rho = 0)} = 0.8 \quad (1)$$

where m_{MV} is the mass of vector meson, ρ_0 indicates the nominal nuclear density, 0.16 fm^{-3} , and $\rho = 0$ indicates the vacuum.

Hatsuda and Lee [7], based on QCD sum rule calculations, obtained the spectral changes of the vector mesons in the nuclear medium. Their calculations result in a linear decrease of the masses as a function of density:

$$\frac{m_{VM}(\rho)}{m_{VM}(\rho = 0)} = 1 - \alpha \frac{\rho}{\rho_0}, \quad \alpha = 0.16 \quad (2)$$

While QCD based models predict a large downward shift of the vector meson masses, more “conventional” processes such as in-medium re-scattering predict no change in the vector-meson mass but a substantial increase in the width of the meson. These effects are density dependent, and, if present, should be observed at normal nuclear densities. Consequently, one should be able to observe the medium

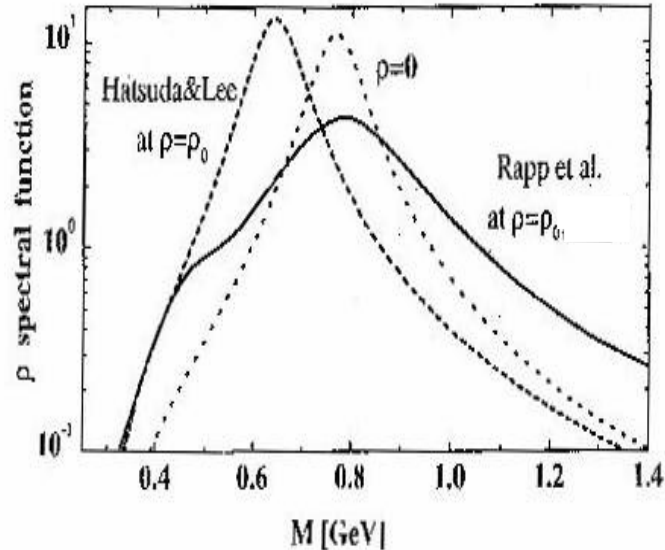


Figure 2: Prediction of Hatsuda and Lee [7] (dashed line) and Rapp *et al.* [9] (solid line) for the mass of the ρ meson at $\rho = \rho_0$ compared to mass of ρ meson at $\rho = 0$ (dotted line).

modifications of the properties of the hadrons in pion-, proton- or photon-induced reactions. Models based on nuclear many body effects predict a broadening in the width of the ρ meson with increasing density. This prediction is based on the assumption that many body excitations may be present with the same quantum numbers and can be mixed with the hadronic states [8, 9]. Fig. 2 shows the prediction of Rapp *et al.* [9] compared to that of Hatsuda and Lee.

1.3 Existing Data

A large downward mass shift has been reported for the ρ meson by the TAGX collaboration, which used photons incident on a ^3He target and detected the $\pi^+\pi^-$ pairs stemming from sub-threshold ρ production [10]. Fig. 3 shows the $\pi^+\pi^-$ invariant mass for different photon beam energies. The fits include all the “non- ρ ” processes (all the processes that contribute to the $\pi^+\pi^-$ channel that are not from decay of the ρ -meson), medium modified ρ mass processes, and ρ mass processes at normal density ($m_{\rho^0} = 768 \text{ MeV}/c^2$). The best fits were obtained with a medium modified

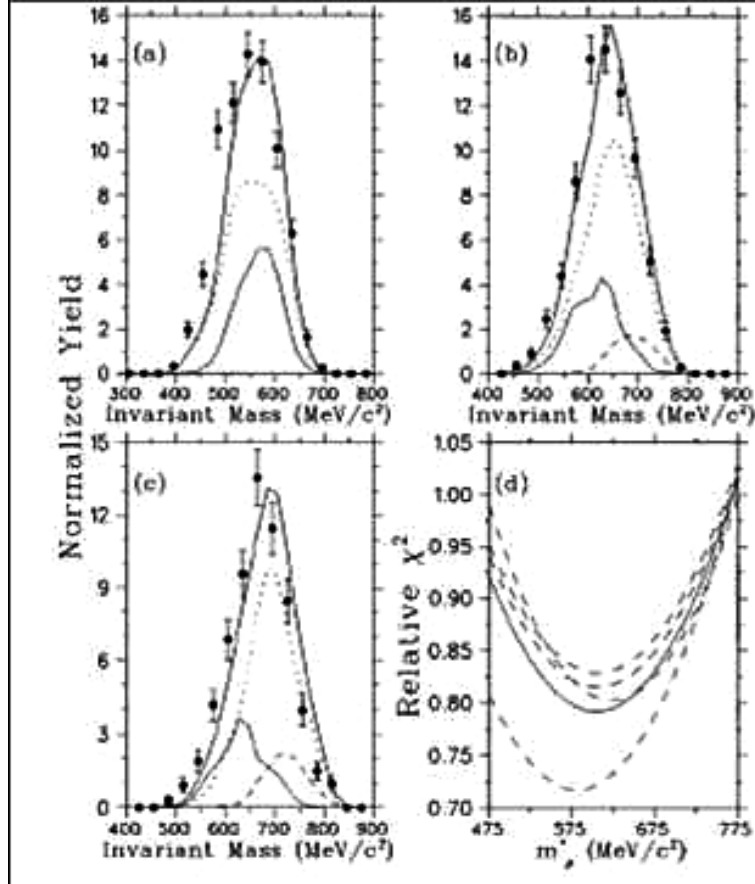


Figure 3: TAGX result. Panels (a)-(c) show the data distribution for $\pi^+\pi^-$ invariant mass for a tagged photon energy beam of (a) 800-880, (b) 960-1040, (c) 1040-1120 MeV. The dotted lines indicate the sum of non- ρ processes; the dashed lines are due to the $m_\rho = 768$ MeV/ c^2 processes; while the lower solid line assumes $m_{\rho^*} = 600$ MeV/ c^2 . The upper solid line is the sum of all the Monte-Carlo fits. Panel (d) shows the χ^2 of the fitting as a function of m_{ρ^*} for the four energy bins. The lowest curve is for 800-880 MeV bin, while the solid curve is the average over all of the photon energies. Data from Ref. [10].

$m_{\rho^*} = 610$ MeV/ c^2 . This corresponds to the maximum Brown/Rho shift expected in the nuclear matter and is a rather large effect for a small nucleus such as ^3He . The $\pi^+\pi^-$ hadronic decay channel is also subject to final state interactions.

An observation of a medium-modified vector meson invariant mass spectrum has been claimed by a KEK-PS collaboration in an experiment where 12 GeV protons were incident on nuclear targets (C, Cu) and the e^+e^- pairs were detected [11, 12]. Fig. 4 shows the invariant mass spectra of e^+e^- obtained in this experiment. Fits

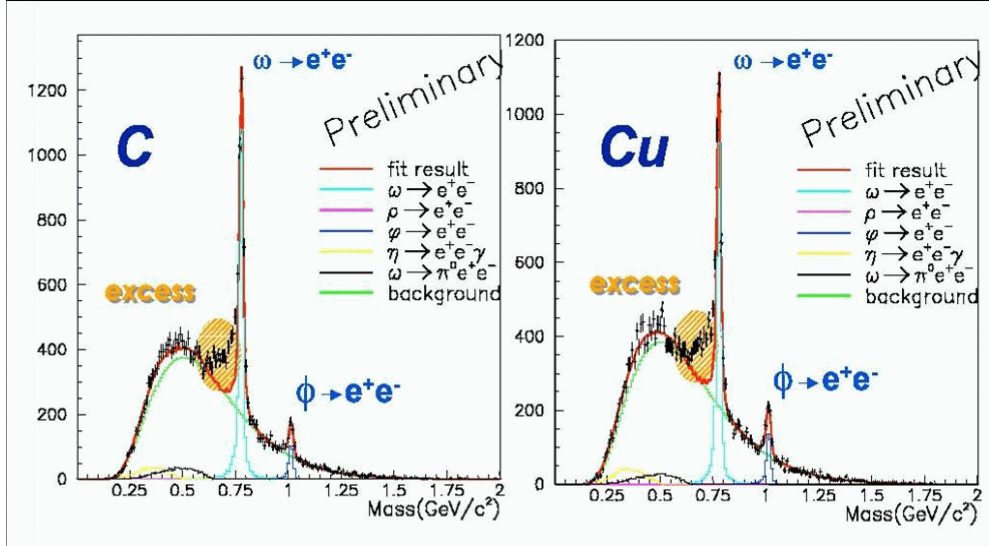


Figure 4: KEK result. Invariant mass spectra of the e^+e^- for C (left) and Cu (right) targets. Best fit results from the mixture of the known hadronic sources and the combinatorial background. Data from Ref. [11]

include all the possible physics processes, the shaded area was excluded from the fit. The background was estimated by mixing leptons from different events. The KEK result does not indicate any contribution from the decay of the ρ meson. It was claimed that ρ mesons are modified in the medium producing the excess mass seen at ω peak shoulder. It is also not possible to conclude any medium effect since the lightest target used as a reference was C. Fig. 5 shows the result of the same experiment for the ϕ meson. It is shown that by selecting low momentum ϕ mesons, the shoulder due to the possibly modified ϕ 's decaying in the nucleus can be enhanced. Since few ϕ 's decay inside the nucleus, one needs sufficient statistics after the momentum cuts to observe the shoulder.

Very recently, the Crystal Barrel/TAPS collaboration has reported a downward shift in the mass of the ω , where the analysis focused on the $\pi^0\gamma$ decay of low-momentum ω mesons photoproduced on a nuclear target [13]. The result of this experiment is shown in Fig. 6. The $\omega \rightarrow \pi^0\gamma$ channel is a very “clean” channel for studying ω mesons since the branching ratio for $\rho \rightarrow \pi^0\gamma$ is two orders of magnitude smaller. Data were taken for two nuclear targets (H_2 and Nb) and compared after

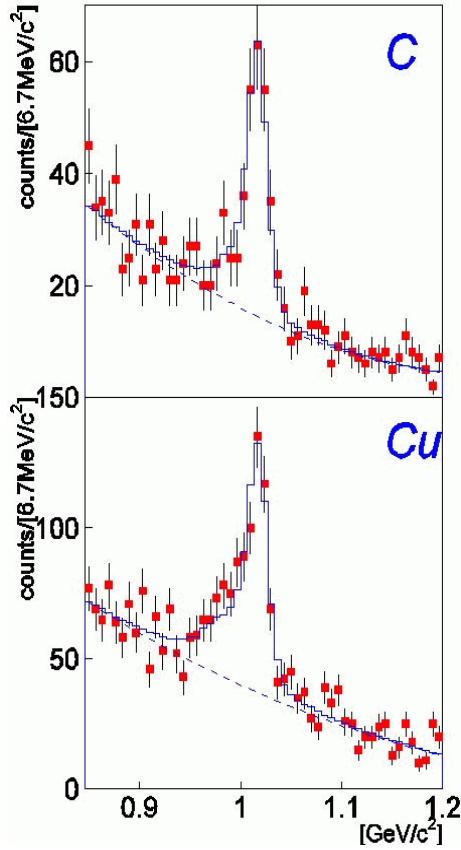


Figure 5: KEK result. Invariant mass spectra showing the low energy ϕ mesons for C (top) and Cu (bottom) targets. Dotted line represent the quadratic background curve. Data from Ref [12].

subtracting the huge background. An enhancement was found toward lower masses for ω mesons produced on the Nb target. Due to the large statistical uncertainties, firm physics conclusions were not possible. The TAPS collaboration is planning to acquire more statistics [14]. One serious concern about this experiment is the possibility of the π^0 re-scattering in the nuclear medium which could distort the invariant mass spectrum.

A recent PHENIX experiment at RHIC also was performed to measure di-leptons in Au+Au collisions [15]. The invariant mass spectrum is shown in Fig. 7 and compared to the expectation from hadronic decays. As shown in Fig. 7, the small signal to background ratio results in large systematic uncertainties that make any physics conclusions impossible.

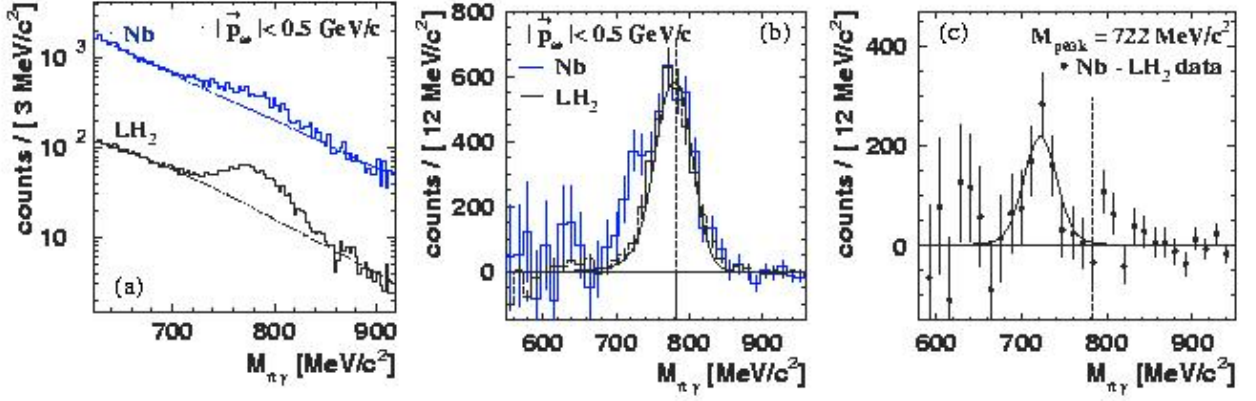


Figure 6: (a) Inclusive $\pi^0\gamma$ invariant mass spectra for momenta less than 500 MeV/c. Upper histogram: Nb data, lower histogram: LH₂ target reference measurement. The dashed lines indicate fits to the respective background. (b) $\pi^0\gamma$ invariant mass for Nb data (solid histogram) and LH₂ data (dashed histogram) after background subtraction. The error bars show statistical uncertainties only. The solid curve represents the simulated line shape for the LH₂ target. (c) In-medium decays of ω mesons along with a fit to the data. The vertical line indicates the vacuum ω mass of 782 MeV/c². Data from Ref. [13].

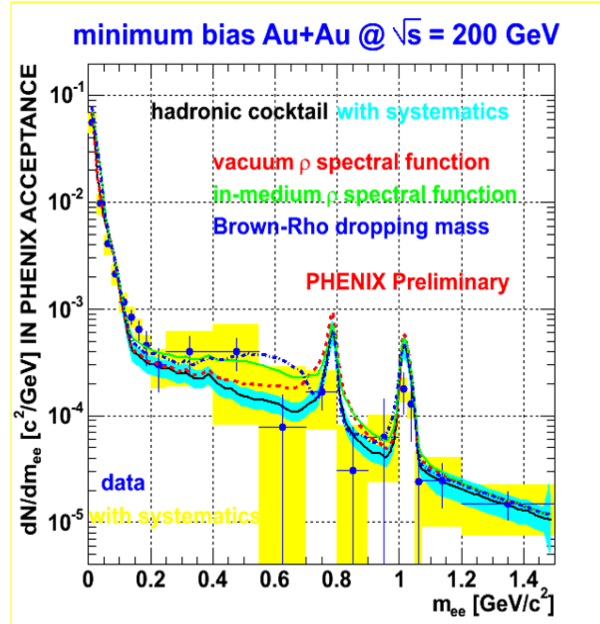


Figure 7: Data (systematic uncertainties shown in yellow) compared to the “cocktail” (systematic uncertainties shown in cyan) and theoretical predictions, where a ρ spectral function is introduced, without (red) and with (blue and green) in-medium modifications. Data from Ref. [15].

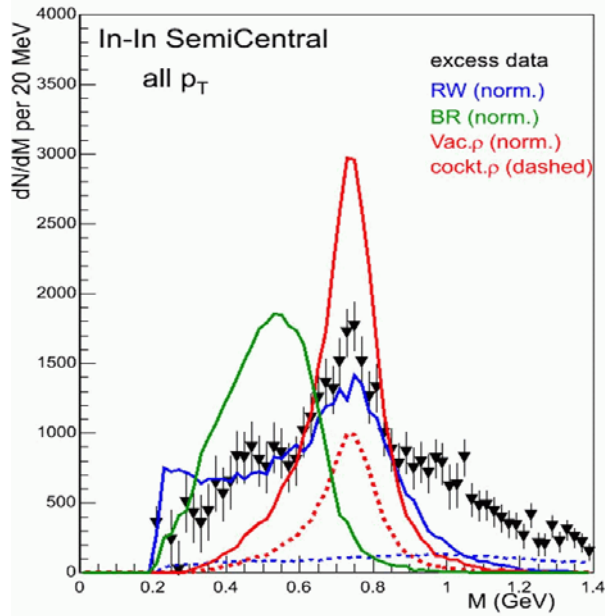


Figure 8: The result of di- μ analysis at CERN SPS. Comparison to model predictions: unmodified ρ (red solid), prediction of Rapp/Wambach [9] for in-medium broadening of ρ (blue solid), in-medium shift by Brown and Rho [6] (green solid), the cocktail (red dashed), and the level of combinatorial charm (blue dashed). Data from Ref [16].

Recently, the NA60 experiment at CERN SPS has studied low-mass muon pairs in 158 AGeV In-In collisions [16]. A strong excess of pairs is observed above the expectation from the neutral meson decays. The high statistics and good mass resolution of about 2% has allowed to isolate the excess by subtraction of the known sources. The shape of the resulting mass spectrum is consistent with a dominant contribution from $\pi^+\pi^- \rightarrow \rho \rightarrow \mu^+\mu^-$ annihilation. The associated ρ spectral function compared to the prediction of the Rapp/Wambach for broadening, and that of Brown/Rho for the shift in the mass of the ρ shows no shift in mass but broadening in the width of the ρ (Fig. 8). However, in their recent paper, Brown and Rho have pointed out that the comparison between the recent NA60 di- μ data as presented is not founded on a correct interpretation of the prediction of Brown and Rho scaling as formulated in 1991 and modernized recently and hence the conclusion drawn by NA60 group is erroneous.

Another study of in-medium ρ meson spectral function in nuclear matter in

TAGX was recently presented at HADRON 2005 workshop [17]. This analysis indicates a large longitudinal polarization for the produced ρ and this signature is used to extract the in-medium ρ invariant mass and its spectral function. The result of this analysis is consistent with some phenomenological models for light nuclei and are also consistent with an observed and significant in-medium mass modification.

The latest medium modification results reported by RHIC experiments are not consistent with the KEK and TAPS conclusions. In heavy ion reactions, the final e^+e^- yield is the result of contributions from different densities and temperatures; thus a discrimination between different scenarios of in-medium modifications for vector mesons is difficult. Experiments such as g7 that look for medium modifications in normal nuclear density at equilibrium are needed to disentangle the different mechanisms [18]. The study of the density-induced modifications on the properties of vector mesons has seen much theoretical and experimental interest. While these experiments are intriguing, no definitive result has yet been obtained, and the question is still wide open.

1.4 Advantages of g7 Experiment

The goal of the JLab g7a experiment was to study properties of vector mesons propagating in nuclei. At JLab energies, photoproduction of ρ -mesons off heavy nuclei is the ideal way to determine any modification of meson properties in nuclear matter (mass shift and/or width increase). Due to their electromagnetic character, di-leptons leave the interaction region without further strong interactions, and thus carry undistorted information of the dynamical properties of the system. Although vector mesons preferentially decay into mesons, the large final state interactions of the mesons with the nuclear medium makes it almost impossible to derive any direct information about the vector meson properties in the medium. A semi-classical BUU transport model calculation by Effenberger and Mosel indeed shows that the $\pi^+\pi^-$ invariant mass spectrum exhibits almost no sensitivity to medium modification of the ρ meson [19]. Even though the branching ratio to e^+e^- is 5×10^{-5} , the predicted in-medium effects for the vector mesons by the different models are so large that they have observable consequences even at normal nuclear density. Effenberger and Mosel have developed a semi-classical BUU transport approach model that is an important first step toward a consistent theoretical description of medium modifications observed in different reactions. This model calculates inclusive particle production in heavy-ion collisions from 200A MeV to 200A GeV, in photon, and in pion induced reactions with the very same physical input. This model has been used to give predictions for di-lepton production in πA reactions that will be measured by the HADES Collaboration, and in γA reactions in the energy range from 800 MeV to 2.2 GeV [20, 21].

The g7 experiment has the advantage of using a photon beam to produce and study the in-medium properties of vector mesons that provides minimum perturbation in the incoming channel. Furthermore, the photoproduction of the vector mesons takes place throughout the nucleus. In the KEK experiment, no definite conclusion about the ρ channel can be made since this channel is barely observed. In the g7 experiment we are able to observe and study the ρ meson. We will be able

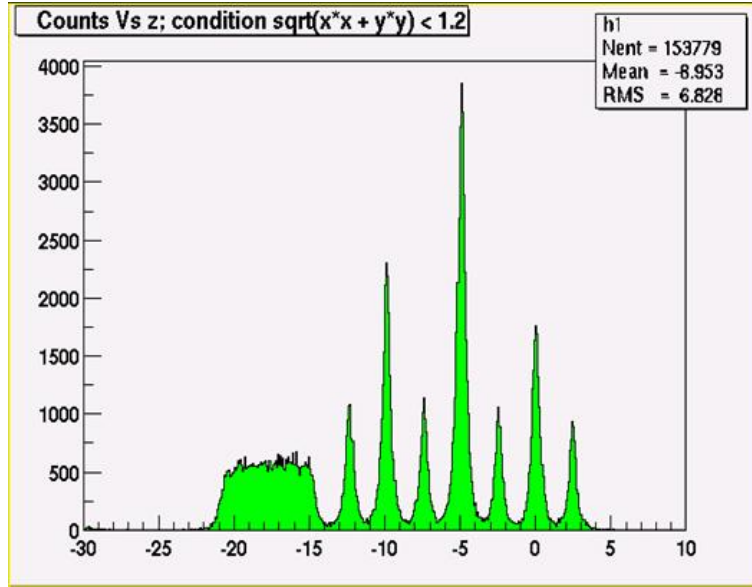


Figure 9: Distribution of the z-component of the reconstructed vertex position for the g7a data. The CLAS vertex reconstruction resolution is about 0.3 cm.

to give a quantitatively measure of the medium modifications, if there are any, given the increased statistics of the g7b experiment. Another advantage of g7 is that we can see and study all three channels of vector meson production (ρ , ω , and ϕ) at the same time.

In the g7a experiment, the $A(\gamma, e^+e^-)A'$ reaction was measured by identifying the coincident electron/positron pairs in the CLAS detector. Energy deposition in the electromagnetic calorimeter and the Cerenkov counter signal define clear cuts for the separation of the e^+e^- events from the very large hadronic background. To minimize systematic errors, the solid targets were divided into several parts, and the separation between adjacent targets (2.5 cm) was matched to the CLAS vertex reconstruction resolution which is 0.3 cm (see Fig. 9).

The data were taken on four nuclear targets simultaneously: deuterium, carbon, iron and lead with a beam intensity of 5×10^7 tagged photons per second in the energy range 1.2 to 3.8 GeV. Setting the magnetic field of the CLAS detector to half its maximum value was found to be optimal for this photon energy range. Tagged photons were used to determine the kinematics of the reaction. In the off-

line analysis, the e^+e^- mass spectra are being analyzed under different kinematical conditions. Bethe-Heitler (e^+e^-) background is drastically reduced with appropriate kinematical cuts. Extensive simulations show that the acceptance of CLAS does not introduce an experimental distortion of the invariant mass spectrum of the detected e^+e^- pair. The analysis of the g7a data taken in Fall 2002 is nearly completed. However, the first g7 run (g7a) is limited by low statistics because of the tagging of the beam, which was done to understand the reaction and the detector. The next experiment will use an untagged photon beam to provide high statistics, and allows for a precise determination of the mass and widths of all three mesons decaying inside the nucleus. For the ρ mesons which mostly decay inside the nucleus, an untagged run can easily acquire 4-5 times more data allowing to measure at the 99% confidence level any mass shift greater than 20 MeV (See Section 4.4). The high statistics g7 run (g7b) will provide the best unambiguous measurement of medium modifications of the ρ mesons. The study of the ω and ϕ mesons which mostly decay outside of the nucleus, require twice as much statistics as the ρ .

Theorists such as U. Mosel at Giessen, M. Soyeur at Saclay and E. Oset at Valencia, have done extensive work on medium modifications of vector mesons, and are interested in the new proposal. Extensive BUU calculations will be done to optimize the choice of target nuclei. The g7b experiment does not require a high beam energy. The data reduction and analysis can be done rapidly since all the analysis tools have already been developed for g7a. Scientific interaction and discussions with the Relativistic Heavy Ion community at RHIC, CERN, and HADES, as well as with the colleagues at KEK and Bonn, will continue because of the ongoing common physics interest.

In the g7 experiment all three vector mesons can be measured at the same time (in contrast to the KEK experiment, where the ρ meson signal is barely observed). The advantage of the g7a/b experiment is that one can clearly see and study the ρ meson in all targets. The preliminary g7a results seem to favor a downward shift in the mass of the ρ meson; this result will be confirmed and quantified with the g7b experiment. Another interesting feature of the g7 experiment is the depletion of the

ω and ϕ meson yields with increasing the target mass; this depletion happens much faster than the prediction of the Giessen BUU model.

The results and details of g7a data analysis procedures are included in Sec. 3. The original g7 experiment proposal that was submitted to PAC20 is also attached.

The g7a/b experiments are part of a larger program at Jefferson Lab. Recently, Jlab proposal E05-110 in Hall A was approved by an A- rating on the modification of nucleons' properties in the nuclear medium. This Hall A approved experiment aims to investigate the properties of nucleons inside the nuclei via the quasi-elastic scattering off nuclei and study the charge and magnetic responses of a single nucleon [22].

2 Manpower

Spokespersons:

- D. P. Weygand (Jlab) Physics, simulations, trigger, data reconstruction, target, data analysis, particle identification, e/π discrimination, photon beam.
- C. Djalali (USC) Physics, particle identification, e/π discrimination, target, data reconstruction, simulation.
- M. H. Wood (UM) Physics, data analysis, trigger, particle identification, e/π discrimination, simulations, data reconstruction.
- R. Nasseripour (USC-postdoc) Physics, background, particle identification, data analysis, preparation, running, simulations, and data taking.

Other Physicists:

- R. Gothe (USC) Physics
- D. Tedeschi (USC) Physics
- S. Strauch (USC) Physics
- L. Guo (Jlab-postdoc) Physics, trigger, simulations, data analysis, preparation, running, and data taking.
- R. Miskimen (UM) Physics

Graduate Students:

- V. Montealegre (USC), Ph.D. student with thesis on g7b experiment, will be stationed at Jlab and involved (100%) in data analysis, simulation, target, beam, preparation and data taking.

All of the physicists have experience running experiments with CLAS and normalization of the photon beam and collimation. The listed manpower has been involved

in the first g7 experiment and is already familiar with all aspects of GEANT simulation and of calibration and reconstruction of g7 data. The e/π discrimination technique, particle identification and data analysis procedures and corrections are well defined and documented in the g7a analysis-note [23]. There are experts of all the phases and aspects of the proposed extended experiment in our group to be confident that we will be able to successfully run the experiment.

3 Feasibility– Analysis of g7(a) data

3.1 Lepton Pair Identification

The e^- and e^+ are identified by looking for particles that satisfy the electromagnetic calorimeter (EC) and Cerenkov counter (CC) coincidence condition. A combination of cuts on the EC and the CC signals is used to reject other charged particles, mainly pions, from the e^- and e^+ samples. One characteristic behavior of pions in the EC is minimum ionization, independent of their energy. These pions are rejected by a cut on the constant minimum ionization energy of 45 MeV deposited in the EC. Furthermore, leptons produce electromagnetic showers and deposit an energy that is proportional to their energy while pions interact hadronically in EC. Therefore, unlike pions, the energy deposited in the EC by the e^- and e^+ has a linear relationship with their momenta as measured by the drift chambers (DC). Pions are rejected by removing events that do not satisfy this relationship (see Fig. 10 and 11). Since almost 100% of the ρ mesons decay into two pions and the relative branching ratio for the e^-e^+ decay channel is of the order of 10^{-5} , it is therefore crucial to discriminate between e^-e^+ and $\pi^-\pi^+$ pairs. The pion rejection efficiency was determined by using similar cuts on the pure sample of pions from the decay of Λ hyperons to $p\pi^-$ and is found to be of the order of 10^{-4} for one and 10^{-7} for two arms. Events that produce less than 2.5 photoelectrons in the CC are also removed to account for pions and noise in the CC (Fig. 12).

In order to identify the lepton pairs from the decay of vector mesons, a set of cuts is applied on the interaction vertex position and time. Fig. 14 shows the vertex timing cut for e^- and e^+ . Because of the RF structure of the primary electron beam at CEBAF, electron buckets are separated by 2.004 ns. This structure can be recognized in Fig. 14. The diagonal dots are due to e^- and e^+ from the same beam bucket with the corresponding photon having different timing (untagged photon). To ensure that the vertical or horizontal bands (pions) are excluded from the e^- and e^+ sample, the following timing cut is applied: $|\Delta t_{e^-,e^+}| < 1.002$ nsec. An additional test is also done by assigning the mass of pions to electrons and comparing

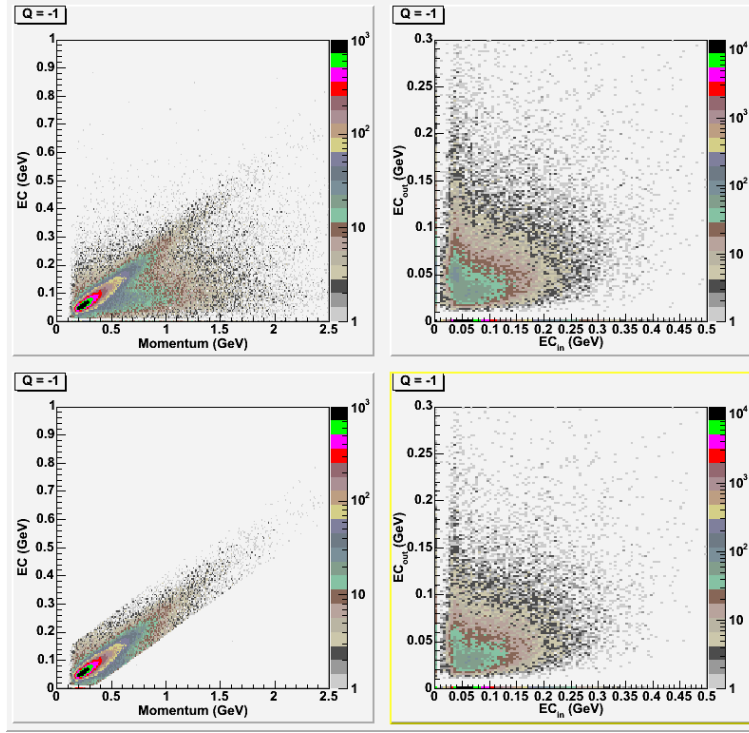


Figure 10: Plots of EC quantities for negatively charged particles. EC versus p (left) and EC_{in} versus EC_{out} (right) before (top) and after (bottom) the EC cuts.

the vertex time. As seen in Fig. 15, when the particle that is labeled as a lepton is given the mass of a charged pion, the vertex timing is smeared out (horizontal bands). However, the true pions, will be assigned the right mass and will show up as the vertical band around zero. It is shown that these misidentified pions are well removed by the above vertex time cut.

The e^+e^- pairs and misidentified pions can also be distinguished by studying the e^+ and e^- SC time where there is no photon timing information required. Fig. 13 shows the e^- versus e^+ SC time. The single band due to the e^+e^- pairs and the two small bands due to the misidentified pions can be recognized.

To express the large opening angle between the e^- and e^+ from the decay of vector mesons, we required pairs to be detected in different sectors of the CLAS detector. This requirement removes the large background from the pairs produced by pair production and Bethe-Heitler processes that have a small opening angle. The remaining background (bump-like structure) around 500 MeV is well modeled

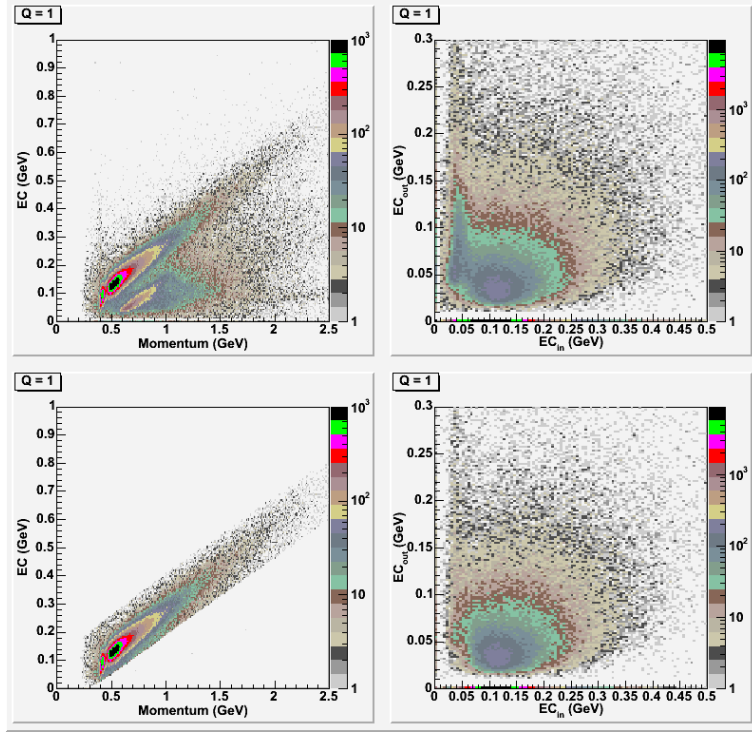


Figure 11: Plots of EC quantities for positively charged particles. EC versus p (left) and EC_{in} versus EC_{out} (right) before (top) and after (bottom) the EC cuts.

by using a the standard mixed-event technique (used by KEK and RHIC). This technique is such that the electron of a given event is combined with the positron of another event (the combined e^+ and e^- are completely uncorrelated), producing a phase space distribution. The shape of the mixed-event distribution matches with the background shape in the invariant mass spectrum for individual targets (Fig. 16). This technique gives the shape of the distribution of the background but not the normalization. Various sources of the mixed event background were investigated by simulating the Compton and pair production processes. The e^+e^- invariant mass distribution where one lepton is from Compton and the other from pair production processes. The obtained invariant mass is very small and therefore this study shows that there are no contributions from mixed leptons from Compton and pair production processes in the region of interest in the invariant mass spectrum, the result is shown in Fig. 18.

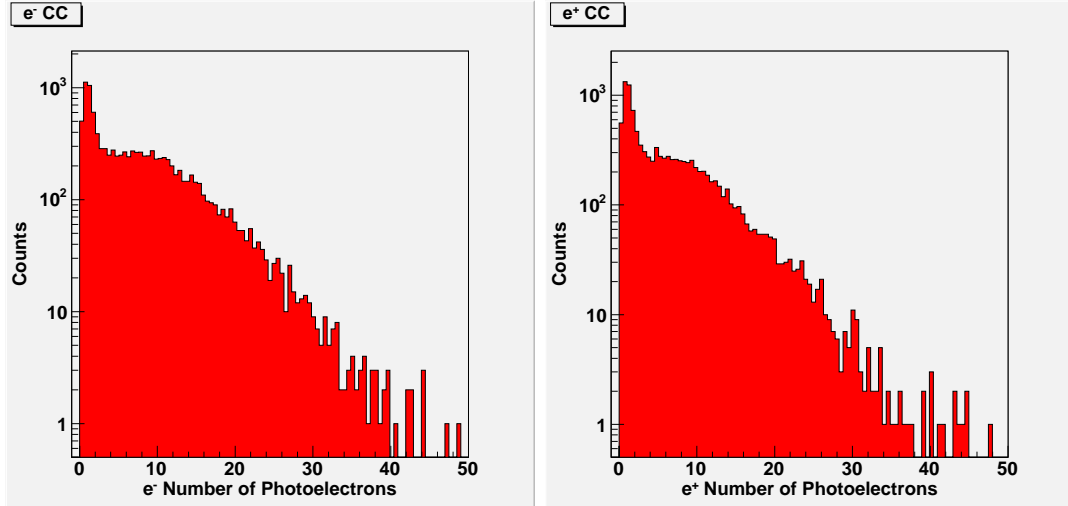


Figure 12: Number of photoelectrons produced in the CC by electrons (left) and positrons (right).

3.2 Momentum and Target Energy Loss Corrections

For various CLAS experiments, it was necessary to adjust the momentum of the detected particles empirically. For this analysis, we have utilized the momentum corrections developed by the g11 run group. The g11 experiment was a Θ^+ search and had very stringent mass requirements. The running conditions were very close to that of g7a. The g11 group also worked very hard at the photon energy determination that is very crucial for studying missing mass. However, it is not important in our study of the invariant mass.

Another correction that must be applied is energy loss in the target. Since the detected particles in the g7 experiment are electrons and positrons, the energy loss is expected to come from ionization.

The average energy loss due to a minimum-ionizing particle is 2 MeV/g/cm^2 of material. Each g7a target was 1 g/cm^2 , and the average energy loss was 0.5 MeV . Table 1 lists the final ω - and ϕ -meson masses and widths after the momentum and energy loss corrections. Both are consistent with the PDG values within statistical uncertainties.

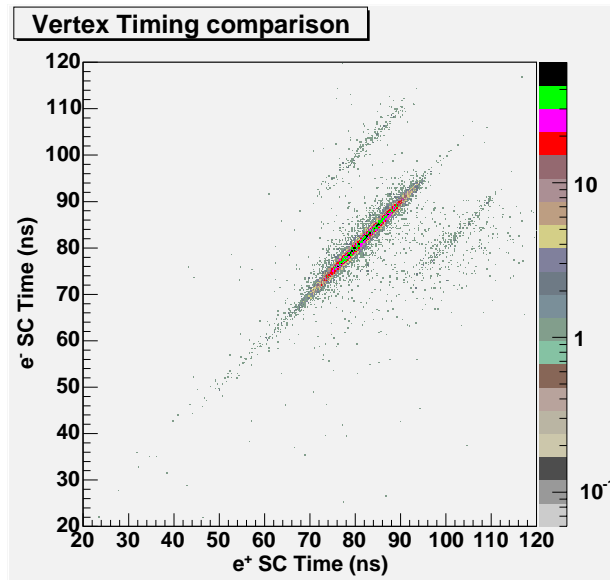


Figure 13: Electron SC time versus positron SC time (ns). The two small bands are due to the misidentified pions while the single big band shows the e^+e^- events. The e^+e^- pairs and misidentified pions can be distinguished with no photon timing information required.

3.3 Simulations and Detector Acceptance

To simulate each physics process, a realistic model was employed and corrected for CLAS acceptance. The events were generated using a code based on a semi-classical Boltzmann-Uehling-Uhlenbeck (BUU) transport model. The code has been developed over many years by the group of U. Mosel at the University of Giessen [21] (this model is rather complete in its inclusion of the various nuclear effects: the shadowing of the photon-induced reactions, the Fermi motion of the nucleons, the Pauli blocking, the mean field potential inside the nucleus, the Coulomb potential felt by charged particles, the final state interactions of the particles produced during the initial interaction, and collisional broadening of the width of the produced resonances are all carefully integrated). We used the BUU event generator for the purpose of simulating the g7a experiment. The events are propagated through the g7 multi-segment target and the CLAS detector using the GSIM simulation package. Fig. 17 shows the acceptance of the CLAS detector as a function of e^+e^- invariant mass in the region of interest for various targets. The smooth slow-varying accep-

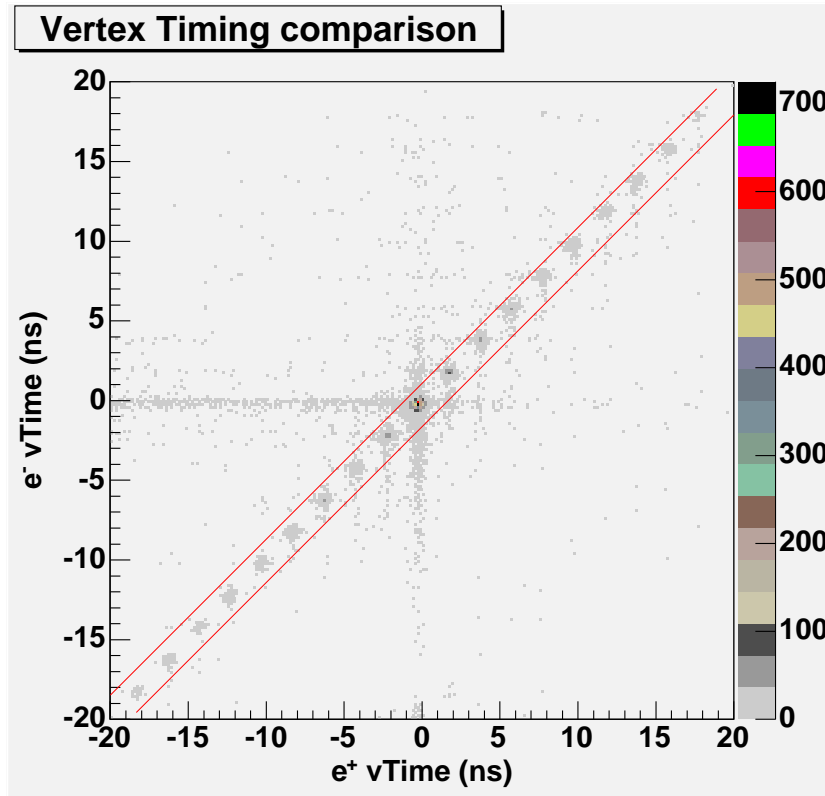


Figure 14: e^- vertex time versus e^+ vertex time. The diagonal dots are due to e^- and e^+ from the same beam bucket with the corresponding photon having different timing (untagged photon). Red lines show the vertex timing cut to remove the misidentified pions (vertical and horizontal bands).

tance does not distort the invariant mass spectrum. Using the BUU transport model for the g7a analysis, one can produce a more realistic acceptance calculation than was previously provided in the g7 proposal in 2001.

Corrections	ω Mass (MeV)	ω Width (MeV)	ϕ Mass (MeV)	ϕ Width (MeV)
None	779.0	11.7	1016	11.8
Momentum	778.9	12.1	1015	11.1
Energy Loss	782.3	13.4	1018	12.1
Both	782.7	13.2	1018	12.3

Table 1: This table lists the masses and widths fitted from the invariant mass spectrum. The PDG values for the ω - and ϕ -meson masses are 782.57 ± 0.12 MeV and 1019.456 ± 0.020 MeV, respectively.

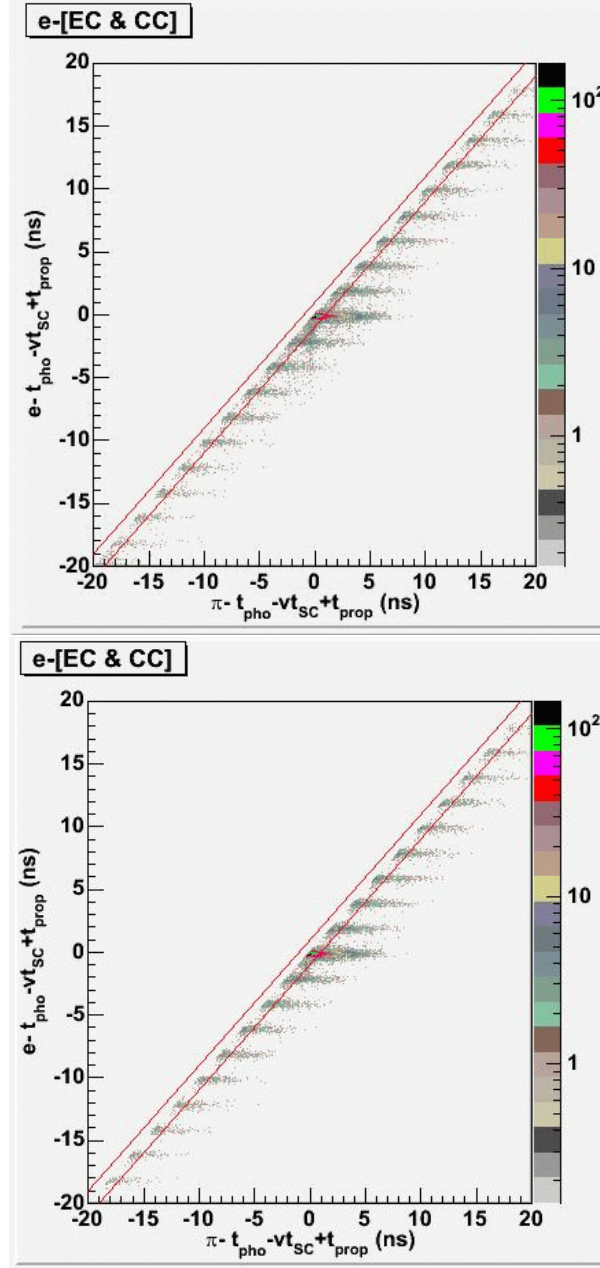


Figure 15: Comparison of vertex timing for e^- with electron mass versus the same quantity where the mass is constrained to that of the π^- before (top) and after (bottom) the e^- and e^+ vertex time. Data are shown in logarithmic scale. The horizontal bands are due to true electrons that are assigned the pion mass. This implies that the particle's vertex timing is best described when the particle is labeled as a lepton, when given the mass of a charged pion, the vertex timing is smeared out. The small vertical band around zero on the top plot are the pions that are misidentified with electrons. These pions are removed after the vertex time cut.

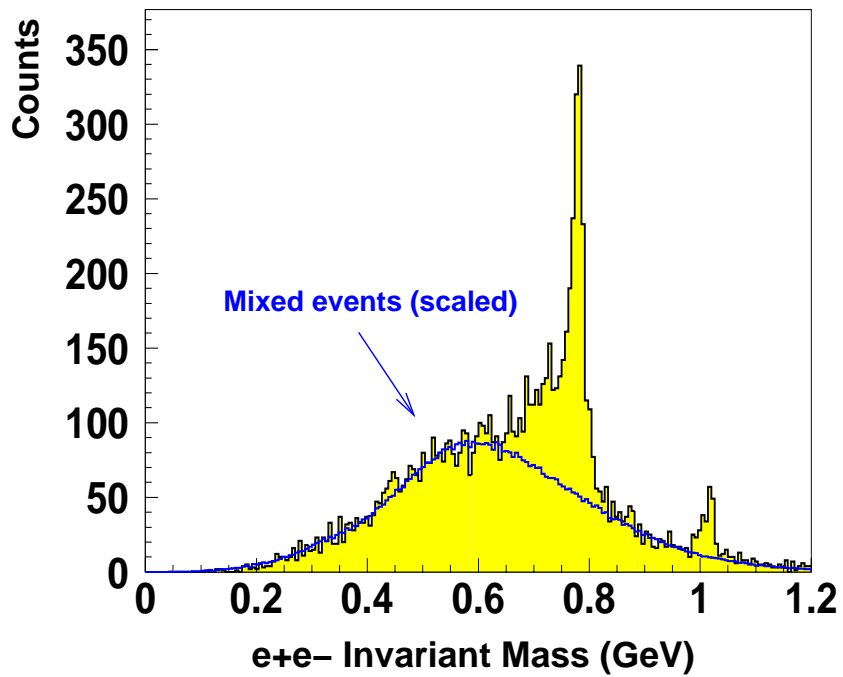


Figure 16: e^+e^- invariant mass (black) with overlaying mixed-event distribution (blue) with arbitrary scaling to match the data. The actual normalization of the combinatorial background is a parameter of the fit (See Section 3.4).

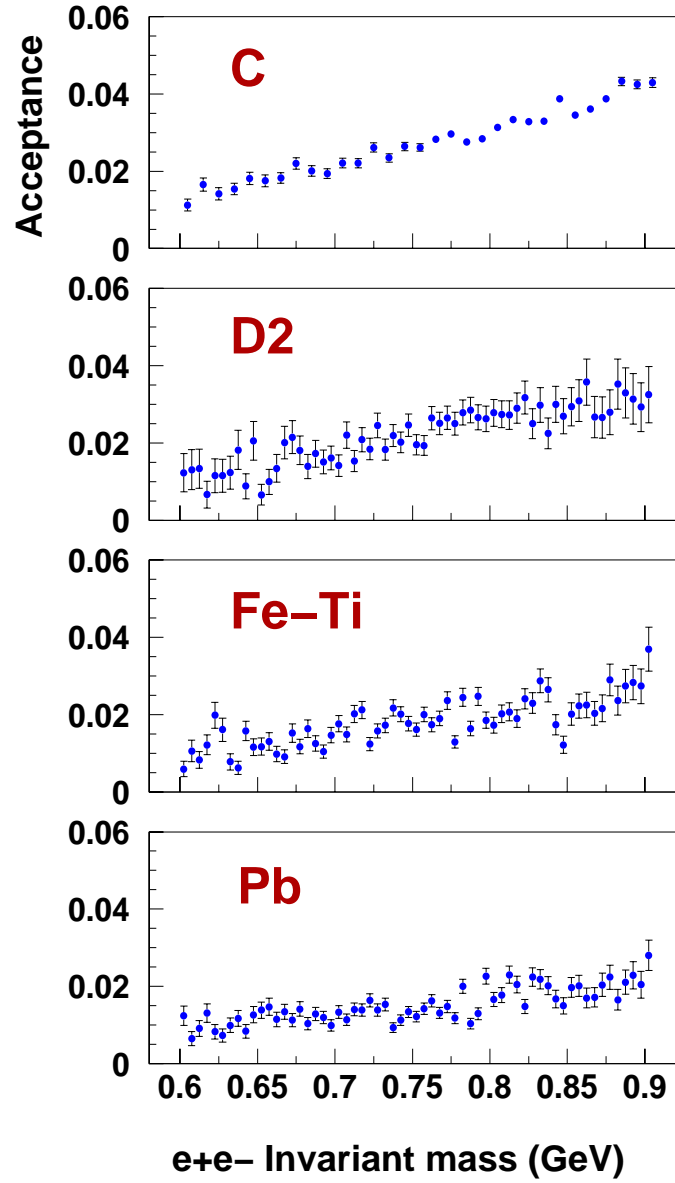


Figure 17: CLAS acceptance as a function of e^+e^- invariant mass for various targets.

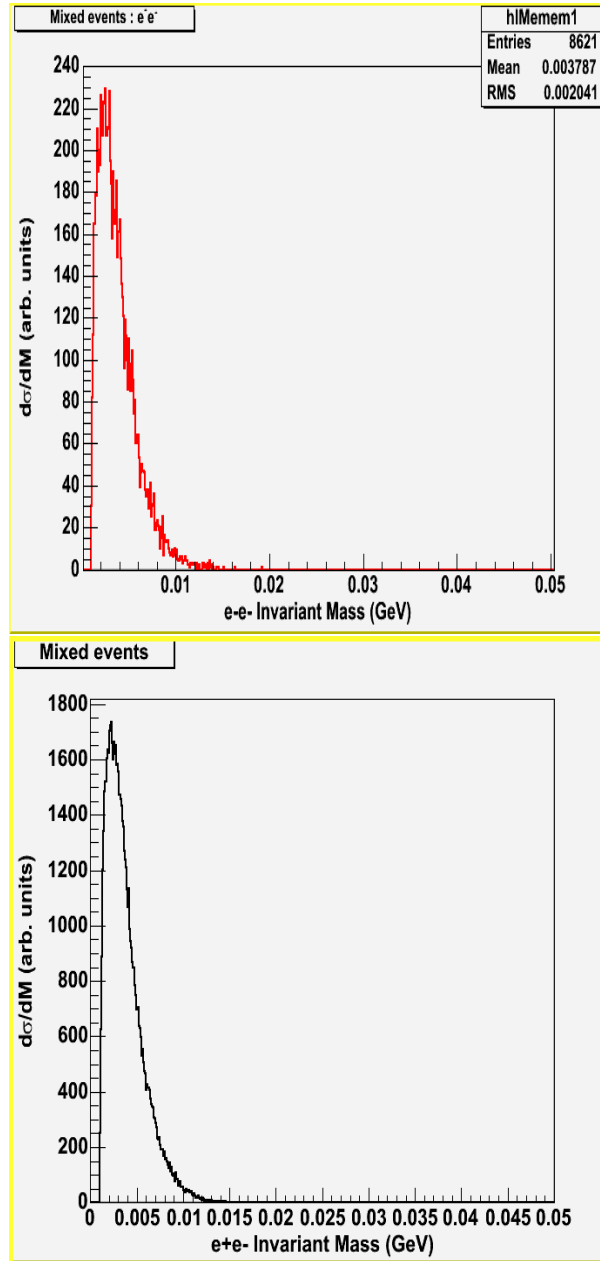


Figure 18: Simulation of mixed e^-e^- invariant mass (top) and mixed e^+e^- invariant mass (bottom) where one lepton is from Compton and the other from pair production processes. The obtained invariant mass is very small and therefore, there is no contribution from this source to our background.

3.4 g7a results

The clear peaks of ω and ϕ mesons can be recognized in the e^+e^- invariant mass spectrum (Fig. 16). It is also shown that the yields of the ω and the ϕ are decreasing with increasing target density (Fig.19 to 22) . The CLAS simulated Monte-Carlo distributions obtained for various possible vector meson decay modes are fit to the e^+e^- invariant mass. Fits are performed with and without incorporating the predictions of Brown and Rho for the vector meson mass shift in the Monte-Carlo model. Note that the BUU code is only used to describe the propagation and decay of the vector mesons in the nucleus. Any medium-induced shift in the mass (Brown/Rho) or width (Rapp/Wambach) of vector mesons, comes from the comparison between different targets, and is derived entirely from the data.

Results of the fits are shown and compared for different targets in Fig. 19 to 22. As seen in the fit results the enhancement at the lower mass of the ω peak may be attributed to the ρ meson. The results of the fits slightly favor a downward shift in the mass of the ρ meson; however, results are also statistically consistent with no mass shift. Unfortunately, the g7a e^+e^- efficiency was smaller than estimated. Therefore, the g7a data set is statistically limited. This makes it impossible to conclude any quantitative measurement on the ρ meson mass shift and/or confirm the prediction of the Brown and Rho model.

Our statistical analysis shows that in order to achieve a 99% confidence level in the χ^2/DOF of the fit, a factor of 4-5 times more data would be needed. The result of the F-test on the fit to the Fe-Ti target data is shown in Fig. 23. The sum of Monte-Carlo distributions (with no mass modifications) obtained from the fits to the data is used as a parent distribution to generate various number of events. The generated events were then fit to the Monte-Carlo distribution with and without including the Brown and Rho predictions. It is shown that the discrimination between the fits to the Monte-Carlo distributions with and without a shift in the mass of the ρ is not possible at the current statistics.

With the planned improvements, the g7b experiment can provide enough statis-

tics to conclude a quantitative physics statement on the in-medium effect on the mass of the ρ .

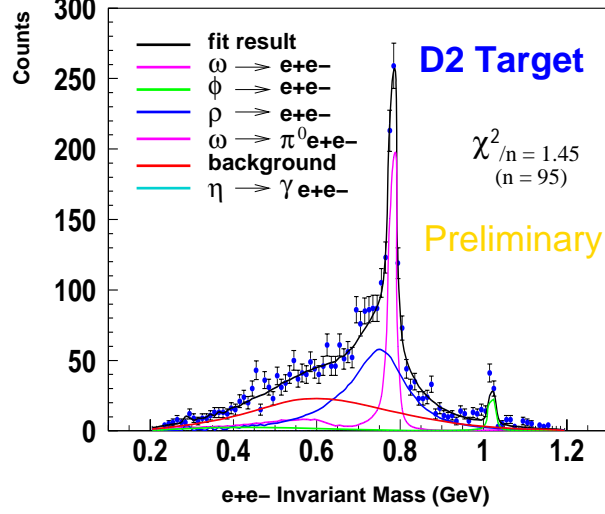


Figure 19: Result of the fits to the e^+e^- invariant mass obtained for D2 data. Curves are Monte-Carlo calculations by the BUU model [19, 20] for various vector mesons decay channels. Background is estimated by the mixed-event technique.

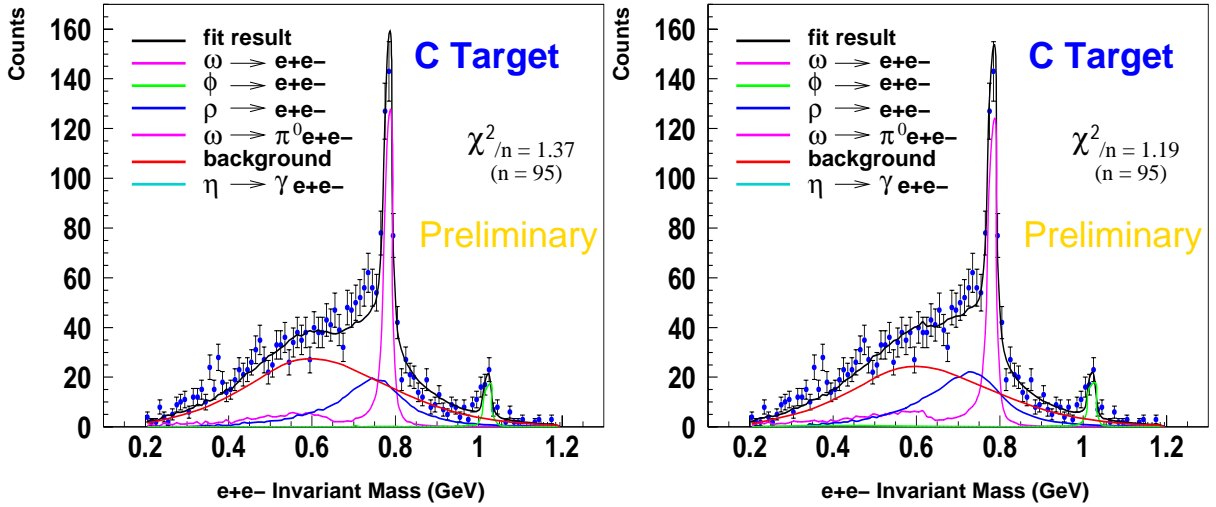


Figure 20: Result of the fit to the e^+e^- invariant mass obtained for C. Curves are Monte-Carlo calculations by the BUU model [19, 20] for various vector mesons decay channels with (left) and without (right) incorporating the prediction of the Brown and Rho [6]. Background is estimated by mixed-event the technique.

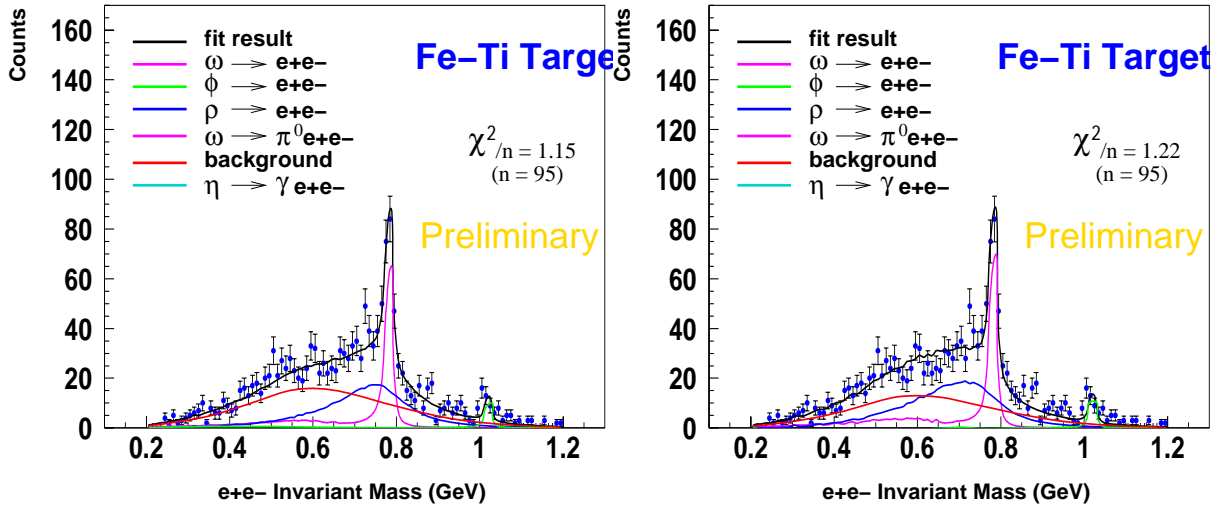


Figure 21: Result of the fit to the e^+e^- invariant mass obtained for Fe-Ti. Curves as described in Fig. 20.

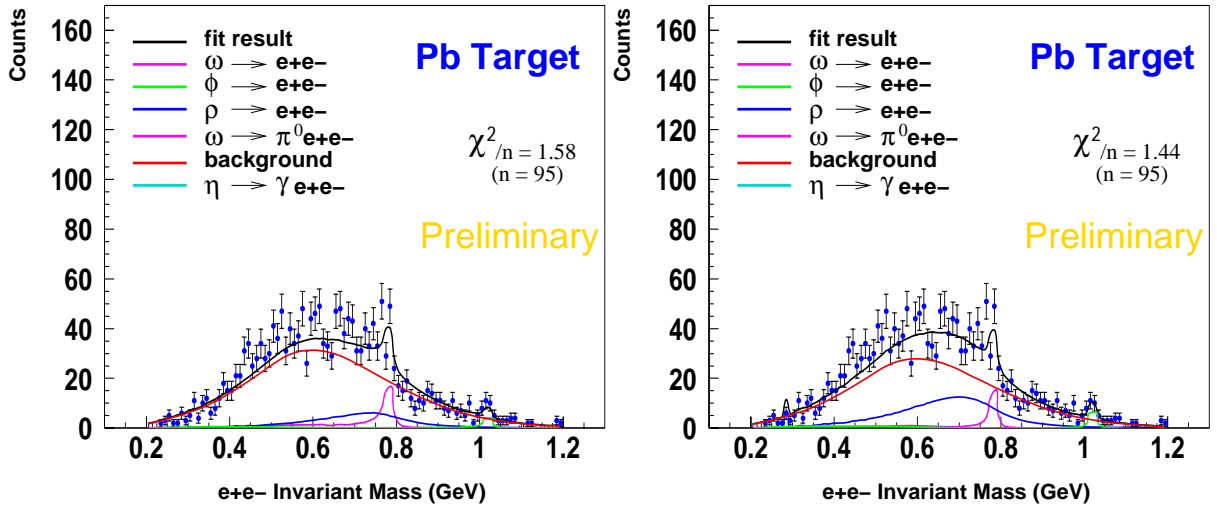


Figure 22: Result of the fit to the e^+e^- invariant mass obtained for Pb. Curves as described in Fig. 20.

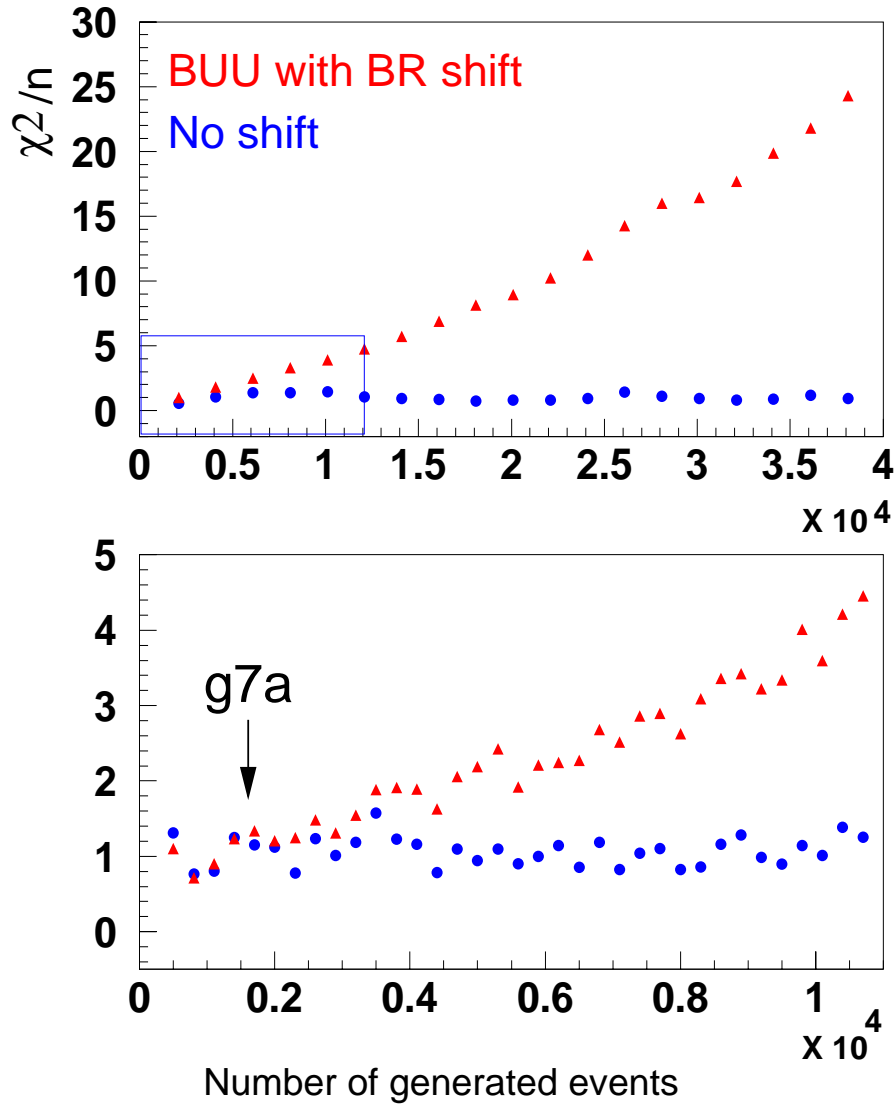


Figure 23: Test of the sensitivity to the mass shift. Top: χ^2/n of the fits as a function of number of generated events. Parent distribution for event generator was obtained from the Monte-Carlo distribution (with no mass shift) fitted to the data. The generated events were fit to the Brown and Rho shifted (red) and not shifted (blue). Bottom: lower left corner of the top plot. With current statistics from g7a, it is not possible to distinguish between the goodness of the fit with and without incorporating the Brown and Rho shift in the Monte-Carlo generator.

4 g7b Running Conditions

The main goal of the g7b experiment is to study the ρ meson which requires increasing the g7a statistics by a factor of 4-5. This can be achieved by a combination of the instantaneous luminosity and the running time. In order to increase the statistics of the g7b experiment compared to g7a, we plan to increase the integrated luminosity by a factor of 4-5 by:

- Run without tagger. (Note that the tagger was not included in the trigger in the g7a experiment. The trigger for the g7a/b experiments is an EC-CC coincidence.)
- increase the thickness of the radiator,
- run for 36 days.

4.1 Data Rate

The g7a trigger rates were about 150 Hz for the 2 lepton trigger and 660 Hz for the single lepton trigger. The maximum rate of the Hall B data acquisition (DAQ) has increased from the g7a value of 3 kHz to 6 kHz today. This improved DAQ rate provides room to increase the data rate for the g7b experiment.

To determine the amount of data needed for g7b, the sensitivity of observing a shift in the mass of the ρ meson was studied as a function of statistics. The procedure to calculate the sensitivity was discussed in Sec. 3.4. Unlike the statistical analysis in Sec. 3.4, where only the Brown/Rho shift was considered, the mass shift was set to 30, 60, or 100 MeV. The result of this statistical analysis is summarized in Table 2. To achieve a 99% confidence level for each shift setting, a factor of 4, 3 or 2 times the g7a data would be needed.

Preliminary results from KEK and TAPS suggest low values of α in the range of 0.12. Therefore, we can see from Table 2 that at least 4 times statistics provides the sensitivity to this range of α .

α	observed shift(MeV) in the ρ mass peak	Number of events	Factor over g7a data
0.13	30	7000	$\times 4$
0.26	60	4500	$\times 3$
0.41	100	3000	$\times 2$

Table 2: The sensitivity of the simulated shift in the mass of ρ as a function of number of generated events with a 99% confidence level in the Fe nucleus with the effective density of $\frac{\rho}{\rho_0}=0.309$.

We propose to increase the instantaneous luminosity by a factor of 2-2.5. For g7a, the average hit occupancy was about 1.2% for Region 1 of each sector in CLAS. Scaling the data rate by a factor of 2 will keep the DC occupancy below 3% which is the operating limits of the CLAS detector.

There are two improvements to the data rate which will be discussed in the Section 4.3.

4.2 Trigger

The triggers for g7b will be the same as the original g7a experiment. In g7a, there were two lepton triggers. The first trigger was set with two lepton tracks which involved hits coincident in the EC, CC, and TOF detectors in two different sectors. The EC and CC components identified the track as a lepton. The TOF component guaranteed that the track was charged and rejected accidental photons in the EC and CC ². The second trigger was a coincidence in the EC, CC, and TOF for one sector. This latter trigger was set for single lepton events and was employed as a systematic check of accidental leptons. The second trigger included the first trigger. For both triggers, a level 2 condition was applied to require at least one track to be identified by the DC. The level 2 requirement was 3 hits out of 5 DC layers .

It should be emphasized that the tagger was not included in the physics trigger logic in g7a. With the g7a flux of $5 \times 10^7 \gamma/s$, the rate in the tagger timing counters was on the order of 50 MHz. The physics trigger rates are on the order of a few hundred Hz. Including the tagger in the trigger would have been ineffective in reducing the data rate. For g7b, we plan again to exclude the tagger from the trigger logic. Since the photon flux will be increased, the tagger counters will be saturated and inefficient at identifying the photon timing.

4.3 g7b Simulations

Simulations were conducted to study the effects of two new improvements: running with the DVCS solenoid instead of the minitorus magnet and replacing the Pb target with a lower Z-material such as Nb or Sn. In both cases, the foam target holder and target spacings were set with the g7a conditions. For the lead shielding just downstream of the target holder, the eg1 design was used. The target holder was moved upstream of CLAS center such that the entrance window of the LD₂ cell was set at -72.94 cm, and the last solid foil target was at z=-49.24 cm. The targets were moved upstream to fit with the position of the DVCS solenoid magnet which

²The trigger requirement was 3 out of 4 EC-CC elements.

was centered at -76.683 cm. Finally, the heaviest target was moved to the penultimate position downstream. Since this target will produce the most electromagnetic background, it is reasonable to move it closer to the exit of the CLAS. Thus, the targets are positioned LD₂, C, Fe, C, Ti, C, Pb, and C when viewed from upstream to downstream on the beamline. In the different simulations, Pb is replaced by Nb or Sn.

The simulation software is GEANT-based which has been developed by Pavel Degtiarenko of the Environmental, Health, and Safety division for background studies. Alexander Vlassov of the Hall B Physics division modified the programs to include the DVCS solenoid magnetic field. The following simulations were run

1. The heaviest target is Pb; the solenoid field set to zero.
2. The heaviest target is ⁴¹Nb; the solenoid field set to zero.
3. The heaviest target is ⁵⁰Sn; the solenoid field set to zero.
4. The heaviest target is Pb; the solenoid magnet is on.
5. The heaviest target is ⁴¹Nb; the solenoid magnet is on.
6. The heaviest target is ⁵⁰Sn; the solenoid magnet is on.

For each case, 10⁷ photons were generated at the entrance window of the LD₂ cell with the momentum along the z-axis. The photon energies were generated with a bremsstrahlung distribution from 100 MeV to the g7a/b range. The output from the simulations were any particles which entered the DC region 1. Fig 24 is a drawing of the simulation geometry. Figs 25 and 26 show the particles produced from 1000 photons with the solenoid magnet off and on (cases 1 and 4, respectively).

Table 3 lists the number of particles detected by region 1 for each case.

The simulations confirm a decrease in the number of detected charged particles when the solenoid magnet is on. More simulations will be performed to optimize the target setup with the solenoid magnet. A detailed comparison will be made to determine which is the preferred magnet either the minitorus or the solenoid.

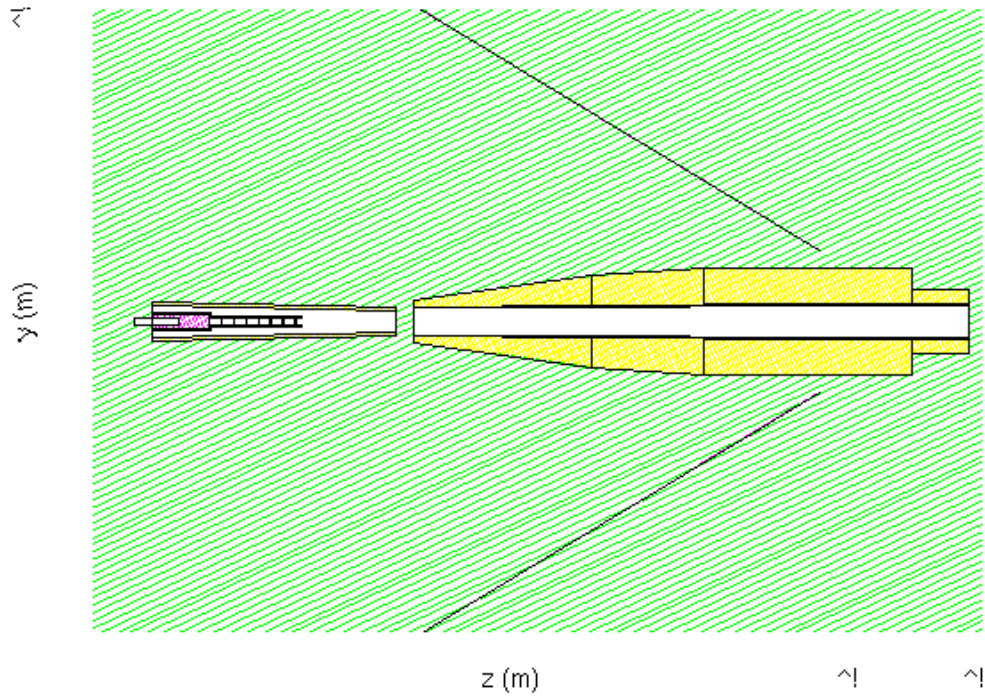


Figure 24: Geometry of the g7b beamline for simulations with the DVCS solenoid.

The more striking result is the reduction in charged particles detected when a lower Z target is inserted. The number of charged particles is cut in half with Nb or Sn and a magnetic field. Thus, using Nb or Sn will reduce the charged particle occupancy in region 1 by a factor of 2.

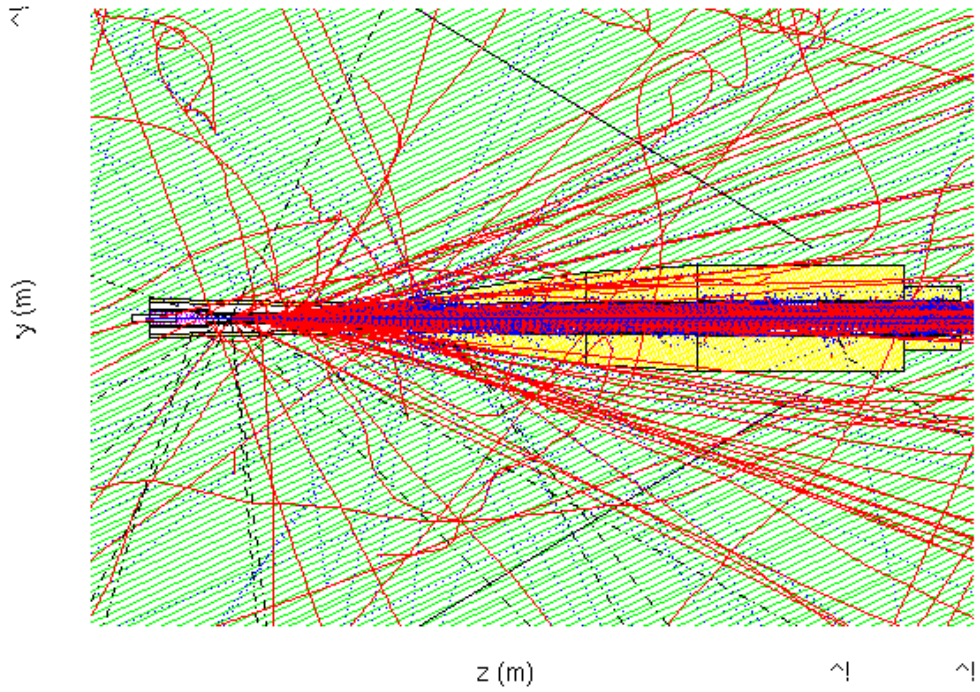


Figure 25: Simulation with the Pb target and with the DVCS solenoid magnet turned off. The number of events thrown was 1000. The red lines are charged particles while the blue lines are photons.

Case	B-field	Heaviest Target	N_γ	N_{e^+}	N_{e^-}	N_Q
1	OFF	Pb	815838	148381	271264	421699
2	OFF	Nb	454615	85460	181337	268535
3	OFF	Sn	503195	94762	193365	289859
4	ON	Pb	836019	70838	82576	156276
5	ON	Nb	458038	32607	39428	73842
6	ON	Sn	512474	38500	46110	86461

Table 3: Results of DVCS solenoid magnet simulations. For each case, the number of photons, positrons, electrons, and all charged particles is listed. The number of thrown photons was 10^7 .

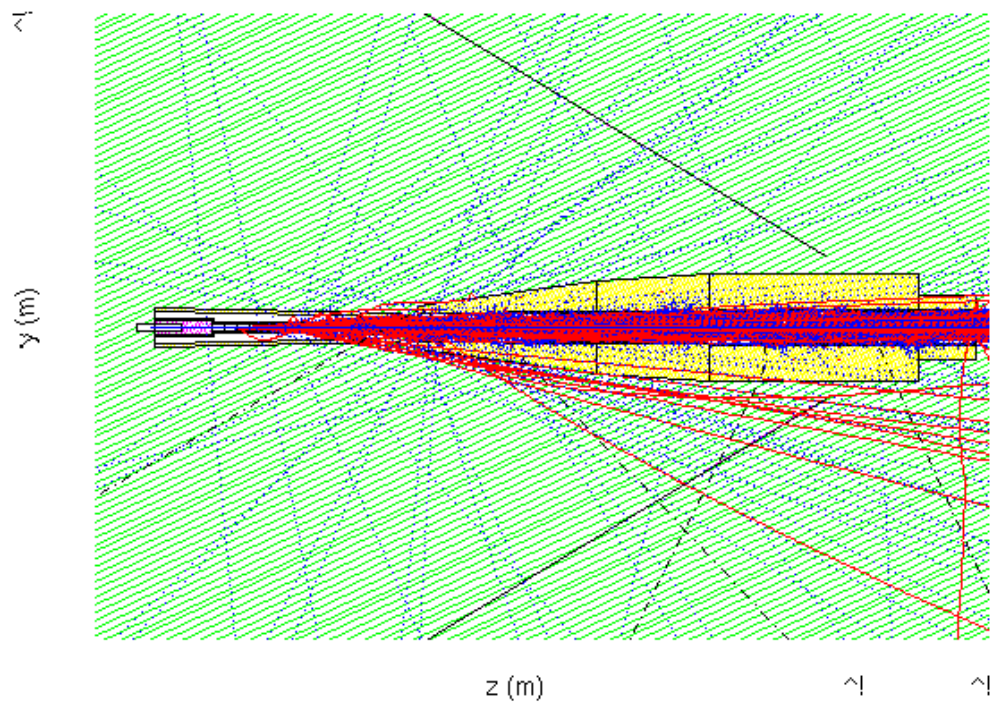


Figure 26: Simulation with the Pb target and with the DVCS solenoid magnet turned on. The number of events thrown was 1000. The red lines are charged particles while the blue lines are photons.

4.4 Background Rates

Scaling the instantaneous luminosity by a factor of 2-2.5 will not increase the accidental rate to a point where the data is swamped by background. Figs. 27 and 28 show the single lepton and two lepton trigger rates as a function of the beam current. From the linear behavior seen in both plots, the trigger rates are not dominated by the accidentals.

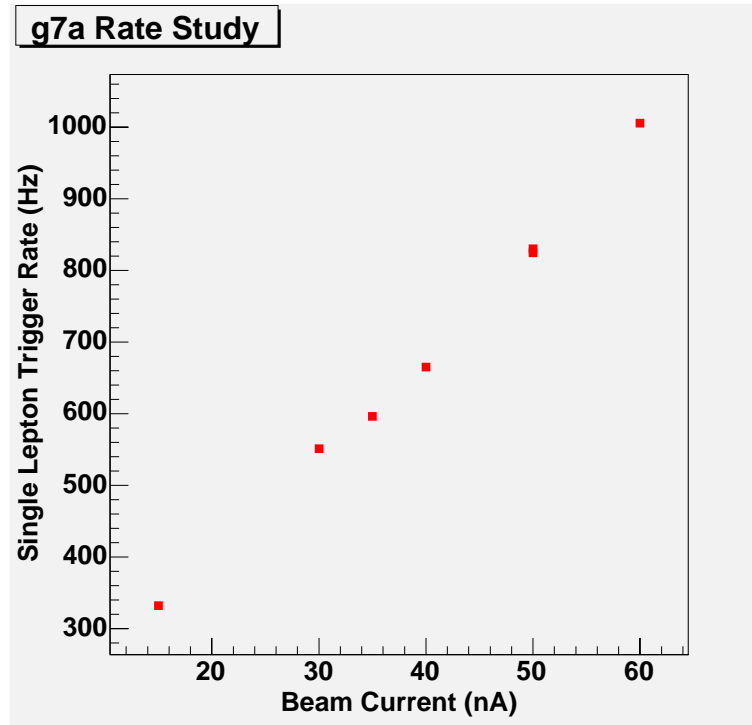


Figure 27: Single lepton trigger rate for g7a data as a function of beam current.

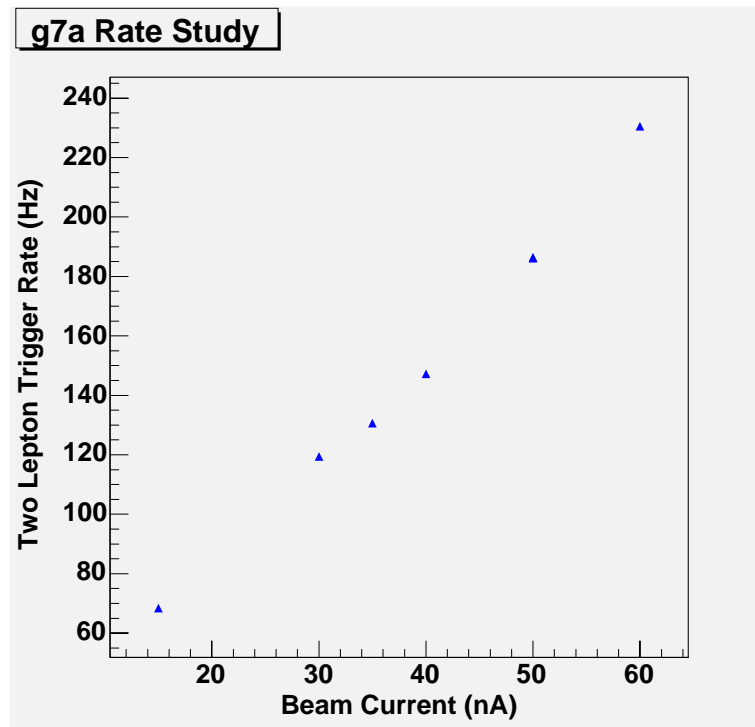


Figure 28: Two lepton trigger rate for $g7a$ data as a function of beam current.

4.5 g7b Target Geometry

The multi-segment g7a target contains material with different average densities. It consists of a cell of liquid deuterium (LD_2) and seven solid thin foils of C, Fe, Ti, and Pb, each contain 1 g/cm^2 material. Four carbon targets were used in g7a experiment to study the effect of vertex position and CLAS acceptance. We plan to reduce the number of foils from seven to four including only C, Fe, Cu, and Nb (or Sn). Replacing Pb with Nb (or Sn) will significantly reduce the background. The spacing between the targets can also be increased for a better vertex resolution and to reduce multiple scattering. The D_2 target will be still used since the small D_2 nucleus is a good reference where no major density-dependent effect is expected. The D_2 target has contributions from both the proton and the neutron compared to H_2 and includes some Fermi motion inside. Furthermore, the same amount of LD_2 takes less space than LH_2 and allows enough space in the scattering chamber to put the other solid foils and separate them sufficiently to avoid multiple scattering effects.

4.6 Photon Beam Energy

As mentioned before, one of the advantages of the g7 experiment is the possibility to produce and study all three vector meson channels, ρ , ω , and ϕ . Fig. 29 shows the production of ω and ϕ mesons folded with the beam energy. As shown, in order to produce the ϕ mesons near threshold, a photon beam of 3 GeV is required.

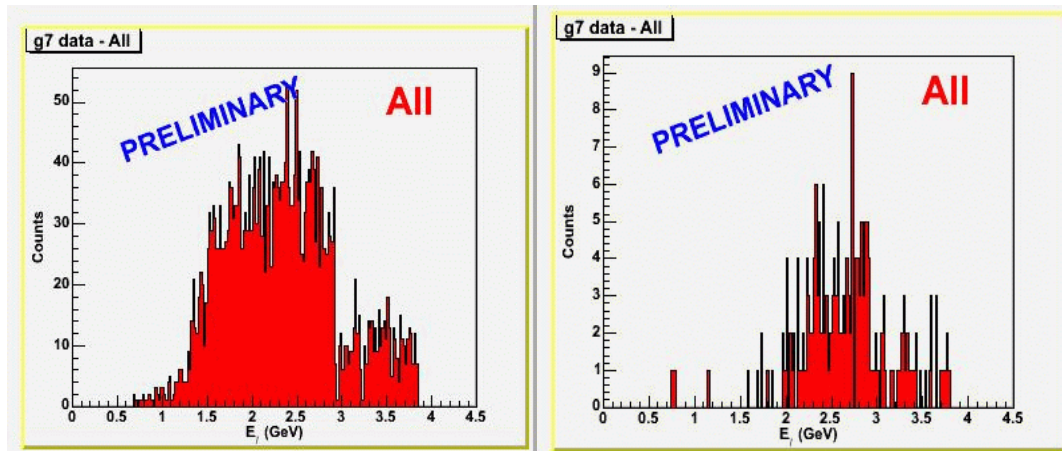


Figure 29: The number of ω (left) and ϕ (right) mesons versus photon beam energy for g7a data. Beam energy required for ω and ϕ meson production near threshold is 3 GeV. Data are shown for all targets.

4.7 Magnetic field settings to optimize the ϕ meson study

The number of ϕ mesons collected by KEK experiment was about 2000, while g7a has an order of magnitude less than that. In order to make a valid comparison on the in-medium modification of the ϕ meson with KEK experiment, a factor of 10 times the g7a data would be needed. This requirement is far more stringent from the running condition of the ρ meson.

The magnetic field setting in CLAS is such that the positrons have outbending tracks. The low-momentum tracks appear at large polar angles and are not detected in the fiducial regions of the EC and CC. Since the electrons bend toward the beamline, these particles have a larger acceptance at low momentum. The result of this acceptance on the lepton momentum is shown in Fig. 30.

In order to reconstruct the low-momentum ϕ mesons, the acceptance of the lower energy positron has to be increased, as the low-momentum vector mesons will have a higher chance to decay inside the nuclear target. Fig. 31 shows the distribution of the lepton pair momentum as a function of the e^+e^- invariant mass for g7a data.

The effect of the torus setting and target position is studied to increase the acceptance for the low-momentum positrons in the g7b experiment. The result of simulations with six different torus settings and 26 target positions are shown in Fig. 32 where the yields of e^+e^- are plotted versus the torus current setting and the z-component of the target position for various decay channels. The distributions of the e^+ and e^- momenta and polar angles were also studied for each torus settings and target positions.

This study shows that the change in the torus setting and target position does not effect the acceptance of CLAS to detect the low momentum e^+e^- pairs. The only way to gain a factor of 10 in the statistics is through increasing the luminosity which is problematic.

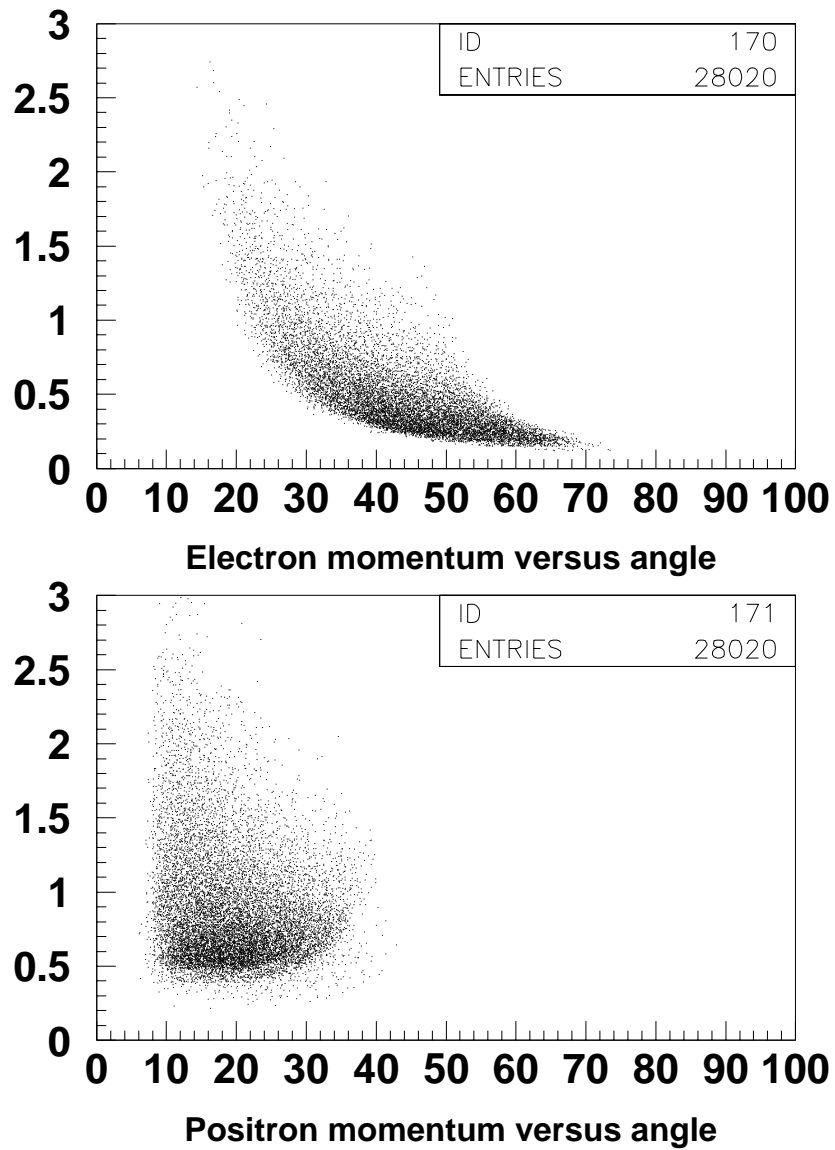


Figure 30: Lepton momentum (GeV) versus polar angle (degrees) for e^- (top) and e^+ (bottom). At the g7a magnetic field setting, the CLAS detector has different angular acceptance for e^- and e^+ at low energy.

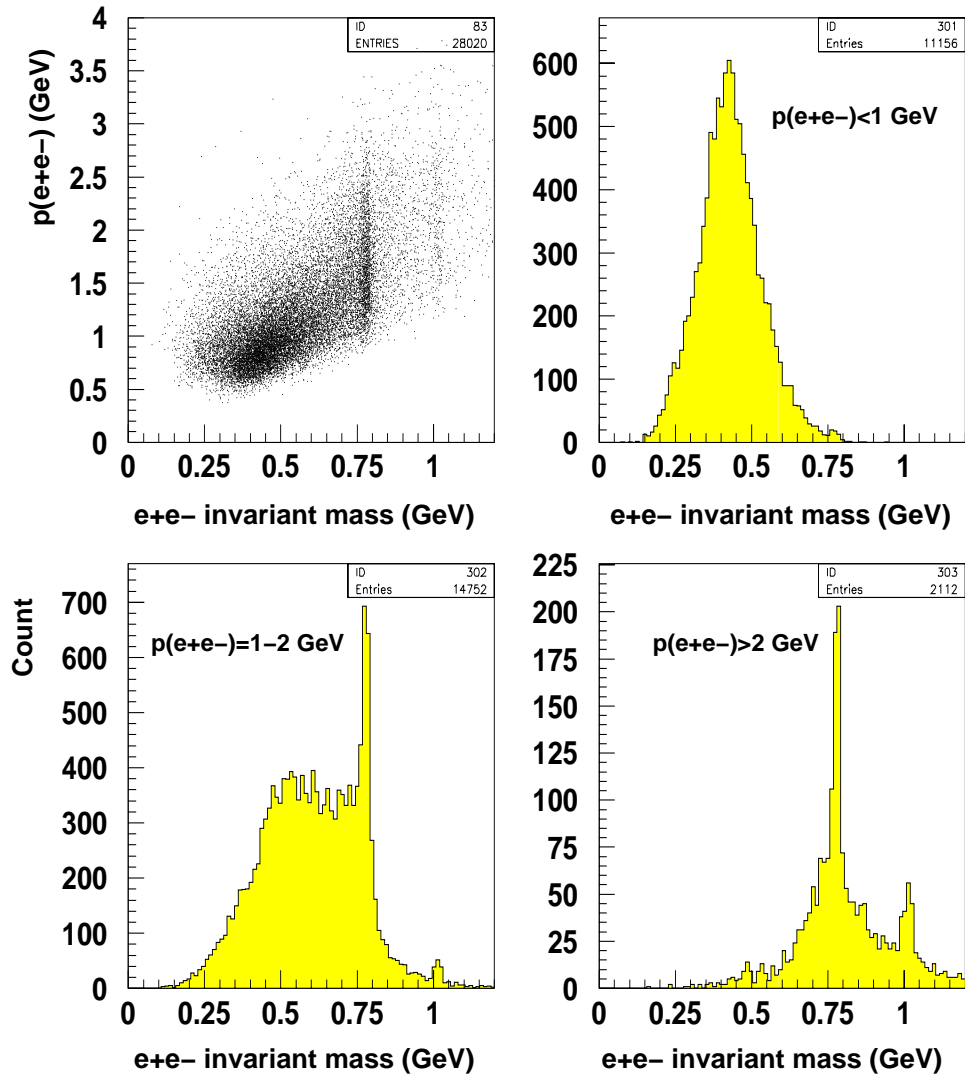


Figure 31: Top: e^+e^- pair momentum versus e^+e^- invariant mass (left), e^+e^- invariant mass shown for pairs momentum < 1 GeV. Bottom: e^+e^- invariant mass shown for pairs momentum $= 1-2$ GeV (left) and pair momentum > 2 GeV (right).

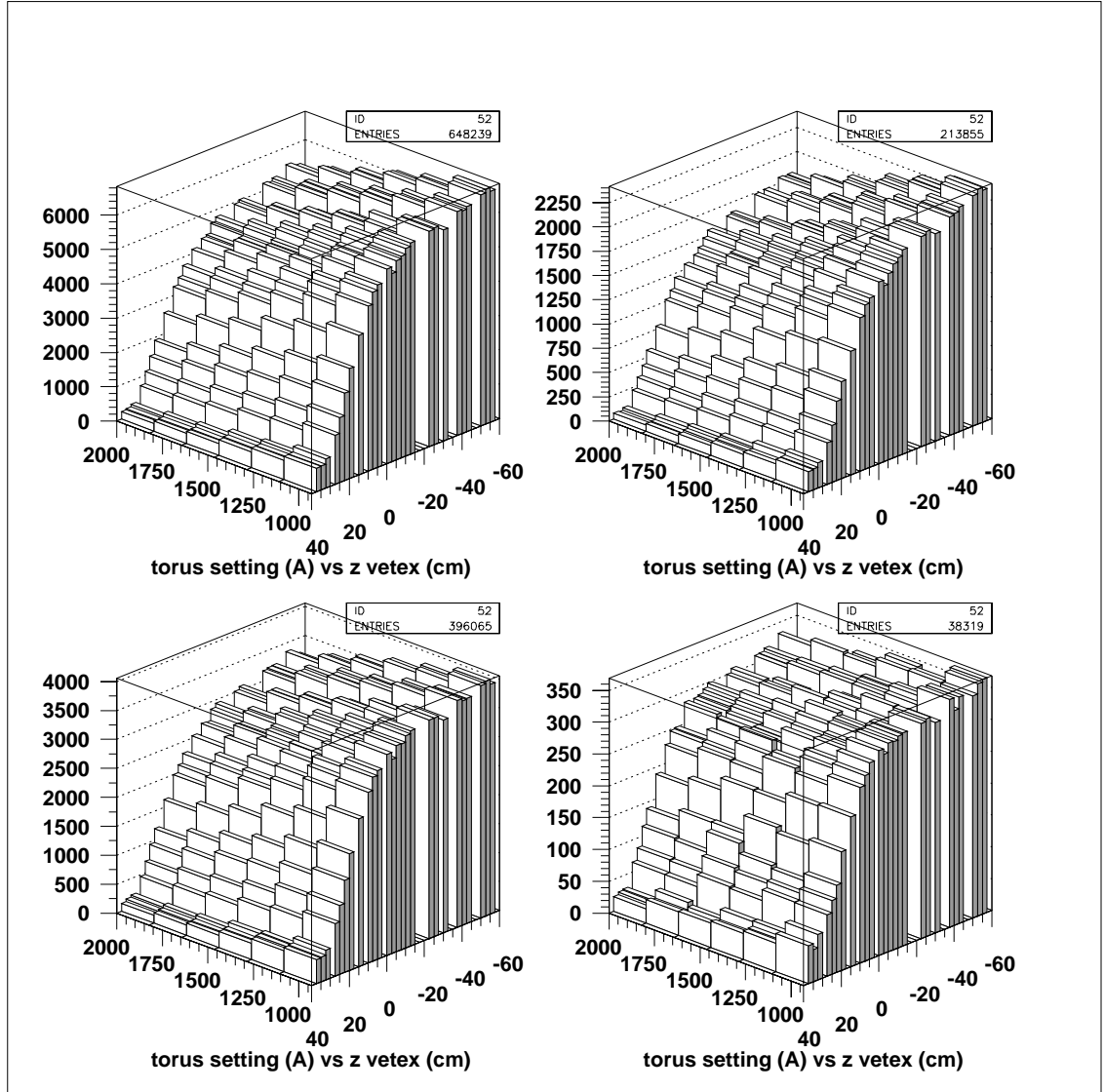


Figure 32: The simulation result showing the yield of e^+e^- pairs for six different torus settings and 26 target positions for all channels (top left), ρ (top right), ω (bottom left), and ϕ channel (bottom right).

5 Summary

In summary, we propose an extension for the g7a experiment (g7b) with a photon beam up to 3 GeV on a set of nuclear targets (D_2 , C, Fe, Nb) using the CLAS detector. The g7a experiment was designed to search for medium modification on the light vector mesons, ρ , ω , and ϕ via their leptonic decay. The result of the analysis on the g7a data has demonstrated the ability to detect the e^+e^- decay of all the three vector mesons.

The extension of the g7a experiment (g7b) is proposed to increase the statistics. Although the result of the fits (with and without medium modification) to the g7a data favor a downward shift in the mass of the ρ meson, it is not possible to draw any statistically significant conclusion. Increasing the amount of data by a factor of 4-5 would make it possible to distinguish between the fit results at the 99% confidence level for the ρ meson. Increasing the statistics also allows a better determination and absolute normalization of the background. This is the primary goal of the g7a/b experiments.

We propose to increase the statistics in the g7b experiment by increasing the instantaneous luminosity and the running time. Increasing the instantaneous luminosity by a factor of 2-2.5 is within the capabilities of the CLAS detector as long as the photon beam is not tagged. The running time of 36 days together with the higher luminosity will give an increase by a factor of 4-5 over the g7a data.

For the ϕ meson, an increase by a factor of 10 is needed to be competitive with KEK results. The CLAS acceptance does not allow us to measure the very low momentum ϕ mesons.

The modification of the fundamental properties of the vector mesons such as mass and width in a dense medium is currently a key component of understanding QCD. While there are a number of experiments investigating in-medium modifications, no definitive result has yet been obtained. The unique characteristics of g7a/b experiment: an electromagnetic probe and a final state unhindered by strong interactions provides a direct measurement of the vector meson properties in the

medium.

6 Acknowledgment

The g7 group would like to thank U. Mosel, P. Muehlich, and A. Afanasev for providing us with theoretical support during this work.

References

- [1] G. Agakichiev *et al.* Phys. Rev. Lett. **75**, 1272 (1995).
- [2] M. Massera *et al.* Nucl. Phys. **A590**, 93c (1995).
- [3] G. Q. Li *et al.* Phys. Rev. Lett. **75**, 4007 (1995).
- [4] C. Song *et al.* Phys. Lett. **B366**, 379 (1996).
- [5] V. Koch and C. Song Phys. Rev. **C60**, 025203 (1996).
- [6] Brown and Rho, Phys. Rev. Lett. **66**, 2720 (1991).
- [7] Hatsuda and Lee, Phys. Rev. **C46**, R34 (1992).
- [8] M. Herrman *et al.* Nucl. Phys. **A545**, 267c (1992).
- [9] R. Rapp *et al.* Nucl. Phys. **A617**, 472 (1997).
- [10] G. J. Lolos *et al.* Phys. Rev. Lett. **80**, 98 (1998).
- [11] R. Muto *et al.* J. Phys. G: Nucl. Part. Phys. **30**, 1023 (2004).
- [12] arXiv:nucl-ex/0511019 v1 8 Nov. 2005.
- [13] D. Trnka *et al.* Phys. Rev. Lett. **94**, 192303 (2005).
- [14] V. Metag, Private communications.
- [15] arXiv:nucl-ex/0510006 v1 Oct. (2005).
- [16] S. Damjanovic *et al.* for the NA60 collaboration, Quark Matter 2005.
- [17] G. Lolos, G. M. Huber, Hadron 2005 workshop.
- [18] G. E. Brown and M. Rho, arXiv:nucl-th/0509001 (2005).
- [19] M. Effenberger and U. Mosel, Phys. Rev. **C62**, 014605 (2000).

- [20] M. Effenberger, E. L. Bratkovskaya, W. Cassing, and U. Mosel, Phys. Rev. **C60**, 027601 (1999).
- [21] M. Effenberger, E. L. Bratkovskaya, and U. Mosel, Phys. Rev. **C60**, 044614 (1999).
- [22] Jlab Proposal E01-016.
- [23] g7a analysis note, <http://clasweb.jlab.org/rungroups/g7/>